

Carbon–Oxygen and Carbon–Hydrogen Bond Cleavage Reactions of *ortho*-Substituted Phenols by Ruthenium(II) Complexes

Masafumi Hirano,* Hiromi Sato, Naoki Kurata, Nobuyuki Komine, and Sanshiro Komiya*

Department of Applied Chemistry, Graduate School of Engineering, Tokyo University of Agriculture and Technology, 2-24-26 Nakacho, Koganei, Tokyo 184-8588, Japan

Received December 28, 2006

Treatment of $\text{Ru}(\eta^4\text{-1,5-COD})(\eta^6\text{-1,3,5-COT})$ (**1**) (COD = cyclooctadiene (C_8H_{12})) with a monosubstituted phenol $\text{HOC}_6\text{H}_4(\text{R}^1\text{-2})$ ($\text{R}^1 = \text{OMe}, \text{CHO}, \text{CO}_2\text{Me}$) in the presence of PMe_3 gives corresponding oxaruthenacycle complexes formulated as *cis*- $\text{Ru}[\text{OC}_6\text{H}_4(\text{R}^1\text{-2})](\text{PMe}_3)_4$ [$\text{R}^1 = \text{O}$ (**2a**), CO (**2b**), CO_2 (**2d**)] accompanied by the C–O or C–H bond cleavage of the *ortho* substituents. Similar treatments of **1**/ PMe_3 with 2,6-disubstituted phenols $\text{HOC}_6\text{H}_3(\text{R}^1\text{-2})(\text{R}^2\text{-6})$ ($\text{R}^1 = \text{OMe}, \text{CO}_2\text{Me}, \text{CHO}, \text{Me}$; $\text{R}^2 = \text{OMe}, \text{Me}$) also proceed to give *cis*- $\text{Ru}[\text{OC}_6\text{H}_3(\text{R}^1\text{-2})(\text{R}^2\text{-6})](\text{PMe}_3)_4$ [$\text{R}^1 = \text{O}, \text{R}^2 = \text{OMe}$ (**2e**); $\text{R}^1 = \text{O}, \text{R}^2 = \text{Me}$ (**2f**); $\text{R}^1 = \text{CO}_2, \text{R}^2 = \text{OMe}$ (**2g**); $\text{R}^1 = \text{CO}_2, \text{R}^2 = \text{Me}$ (**2h**); $\text{R}^1 = \text{CO}, \text{R}^2 = \text{OMe}$ (**2i**); $\text{R}^1 = \text{CO}, \text{R}^2 = \text{Me}$ (**2j**)]. On the basis of the reaction profiles monitored by NMR spectroscopy, a mechanism involving a cationic η^5 -cyclooctadienylruthenium(II) intermediate, $[\text{Ru}(\eta^5\text{-C}_8\text{H}_{11})(\text{PMe}_3)_3][\text{OAr}]$ (**11**), followed by the carbon–heteroatom bond cleavage is proposed.

Introduction

Bond cleavage reaction by transition-metal complexes is one of the current topics in organometallic chemistry. Among such carbon–heteroatom bond cleavage reactions, cleavage of carbon–halogen bonds in organic halides has been extensively studied and used in organic synthesis because of the facile oxidative addition to low-valent transition-metal complexes. However, these processes eventually eject hydrogen halides or corresponding salts as wastes. To avoid this problem, transition-metal-promoted reactions of carbon–non-halogen element bonds are promising alternatives as environmentally benign non-halogen processes. For this reason, the reactions involving a C–H bond cleavage step by transition-metal complexes are extensively studied, and some of them were applied to catalytic molecular transformation reactions.¹ Carbon–heteroatom bond cleavage reactions are also important fundamental processes in view of molecular transformations. For example, C–O bond cleavage reaction in allylic and vinylic esters and ethers is usually easily promoted by transition-metal complexes probably owing to the proximity of the metal center to the C–O bond via prior coordination of the C=C bond.^{2–5} Alkyl esters and ethers seem to be generally less reactive, as C–O bond cleavage reactions of ethyl phenyl ether and 6-methoxysalicylic acid by typical organic process (i.e., transition-metal complex free processes)

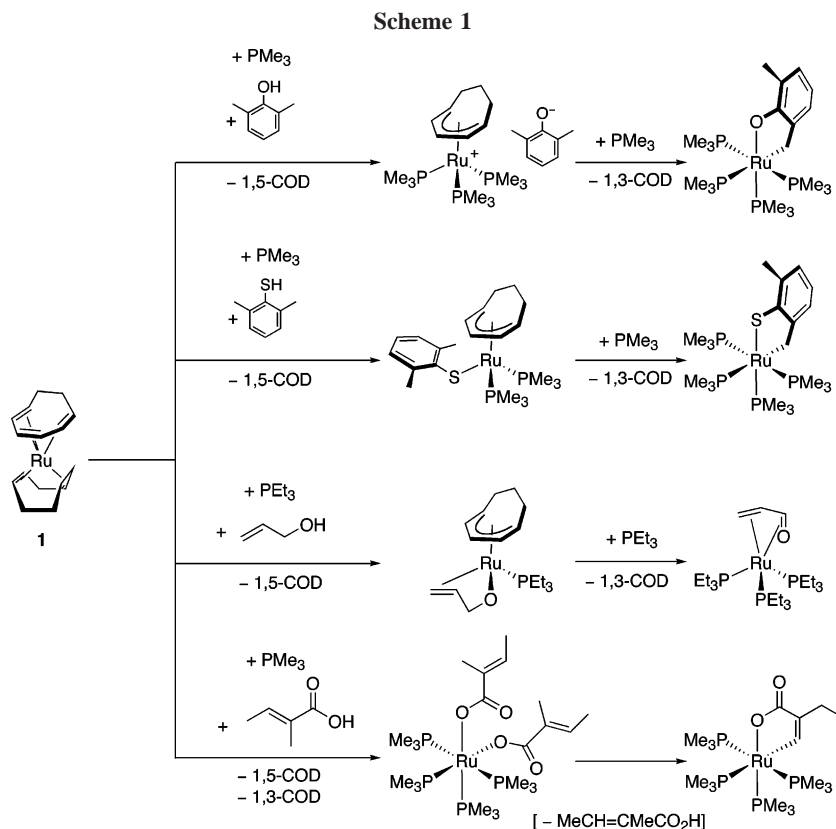
require severe acidic or basic conditions such as reflux in $\text{HBr}/\text{H}_2\text{O}$ and mixtures of KOH/NaOH at 250 °C, respectively.^{6,7} The transition-metal-promoted cleavage reactions of C–O bonds in alkyl or aryl esters and ethers are still limited. Pioneering examples involve the C–O bond cleavage reactions of methyl acetate and methyl benzoate with $\text{FeH}(\text{naphthyl})(\text{dmpe})_2$,⁸ and 6-methyl-2-methoxyacetophenone with $\text{RuH}_2(\text{CO})(\text{PPh}_3)_3$.⁹ These processes are believed to require prior coordination of substrates to the metal center. In fact, introduction of an “anchor” group in the ester or ether facilitates the C–O bond cleavage reactions, for example, N donors in ester in the reactions of $\text{PhCO}_2\text{CH}_2\text{-(2-pyridyl)}$ with $\text{Ru}_3(\text{CO})_{12}$,¹⁰ and 8-acetoxy-2-diphenylphosphinomethylquinoline with $[\text{RhCl}(\text{C}_6\text{H}_{14})_2]_2$,¹¹ and P donors in ether in the reactions of $\text{MeOC}_6\text{H}_3(\text{CH}_2\text{P}^i\text{Bu}_2)_2$ with $[\text{RhCl}(\text{1,5-COD})_2]$ or $\text{Pd}(\text{CF}_3\text{CO}_2)_2$,¹² $\text{MeOC}_6\text{H}_3(\text{CH}_2\text{P}^i\text{Bu}_2)_2$ with NiI_2 ,¹³ and $^t\text{Bu}_2\text{PCH}_2\text{C}_6\text{H}_3(\text{OMe})_2$ with $[\text{PdCl}(\text{2-methylallyl})_2]_2$.¹⁴

We previously reported stoichiometric and catalytic C–H bond cleavage reactions of *ortho*-substituted phenols,¹⁵ benzenethiols,¹⁶ allylic alcohols,¹⁷ and carboxylic acids¹⁸ assisted

* Corresponding authors. Phone and Fax: +81 423 887 044. E-mail: hrc@cc.tuat.ac.jp (M.H.); komiya@cc.tuat.ac.jp (S.K.).

(1) (a) Shilov, A. E.; Shteinman, A. A. *Coord. Chem. Rev.* **1977**, *24*, 97. (b) Crabtree, R. H. *Chem. Rev.* **1985**, *85*, 245. (c) Arndtsen, B. A.; Bergman, R. G.; Mobley, T. A.; Peterson, T. H. *Acc. Chem. Res.* **1995**, *28*, 154. (d) Shilov, A. E.; Shul'pin, G. B. *Chem. Rev.* **1997**, *97*, 2879. (e) Murai, S. In *Activation of Unreactive Bonds and Organic Synthesis*; Springer: Berlin, 1999. (2) (a) Lin, Y.-S.; Yamamoto, A. In *Topics in Organometallic Chemistry*, Vol. 3, Murai, S. Ed.; Springer-Verlag, Berlin, 1999; p 161. (b) Yamamoto, A. *Adv. Organomet. Chem.* **1992**, *34*, 111. (3) Komiya, S.; Hirano, M. In *Current Methods in Inorganic Chemistry: Fundamentals of Molecular Catalysis*; Kurosawa, H., Yamamoto, A., Eds.; Elsevier: Amsterdam, 2003; Vol. 3, Chapter 3, p 115. (4) Amatore, C.; Gamez, S.; Jutand, A. *Chem.-Eur. J.* **2001**, *7*, 1273. (5) (a) Fiaud, J.-C.; Legros, J.-Y. *J. Org. Chem.* **1987**, *52*, 1907. (b) Stary, I.; Kocovsky, P. *J. Am. Chem. Soc.* **1989**, *111*, 4981.

(6) Tiecco, M. *Synthesis* **1988**, 749. (7) Bhatt, M. V.; Kulkarni, S. U. *Synthesis* **1983**, 249. (8) (a) Ittel, S. D.; Tolman, C. A.; English, A. D.; Jesson, J. P. *J. Am. Chem. Soc.* **1978**, *100*, 7577. (b) Tolman, C. A.; Ittel, S. D.; English, A. D.; Jesson, J. P. *J. Am. Chem. Soc.* **1979**, *101*, 1742. (9) Kakiuchi, F.; Usui, M.; Ueno, S.; Chatani, N.; Murai, S. *J. Am. Chem. Soc.* **2004**, *126*, 2706. (10) Chatani, N.; Tatamidani, H.; Ie, Y.; Kakiuchi, F.; Murai, S. *J. Am. Chem. Soc.* **2001**, *123*, 4849. (11) Grotjahn, D. B.; Joubran, C. *Organometallics* **1995**, *14*, 5171. (12) van der Boom, M. E.; Liou, S.-Y.; Ben-David, Y.; Shimon, L. J. W.; Milstein, D. *J. Am. Chem. Soc.* **1998**, *120*, 6531. (13) van der Boom, M. E.; Liou, S.-Y.; Shimon, L. J. W.; Ben-David, Y.; Milstein, D. *Inorg. Chim. Acta* **2004**, *357*, 4015. (14) Weissman, H.; Shimon, L. J. W.; Milstein, D. *Organometallics* **2004**, *23*, 3931. (15) (a) Hirano, M.; Kurata, N.; Marumo, T.; Komiya, S. *Organometallics* **1998**, *17*, 501. (b) Hirano, M.; Kurata, N.; Komiya, S. *J. Organomet. Chem.* **2000**, *607*, 18. (16) Hirano, M.; Sakaguchi, Y.; Yajima, T.; Kurata, N.; Komine, N.; Komiya, S. *Organometallics* **2005**, *24*, 4799. (17) Kanaya, S.; Imai, Y.; Komine, N.; Hirano, M.; Komiya, S. *Organometallics* **2005**, *24*, 1059. (18) Kanaya, S.; Komine, N.; Hirano, M.; Komiya, S. *Chem. Lett.* **2001**, 1284.



by use of chalcogen anchor groups in ruthenium(II) complexes (Scheme 1). Herein we report C–O and C–H bond cleavage reactions of ether, ester, or formyl groups in the *ortho* positions of phenols. The reaction mechanism for the C–O bond cleavage reaction is also proposed.

Results and Discussion

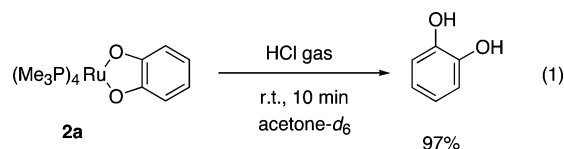
***ortho*-Monosubstituted Phenols.** Treatment of $\text{Ru}(\eta^4\text{-1,5-COD})(\eta^6\text{-1,3,5-COT})(\text{PMe}_3)_4$ (**1**) (COD = cyclooctadiene (C_8H_{12}); COT = cyclooctatriene (C_8H_{10})) with 2-methoxyphenol and PMe_3 in benzene at 70 °C followed by workup procedure including recrystallization from cold toluene gave analytically pure pale yellow needles of the new oxaruthenacycle complex $\text{cis-Ru}[\text{OC}_6\text{H}_4(\text{O}-2)-\kappa^2\text{O},\text{O}'](\text{PMe}_3)_4$ (**2a**) in 15% yield (Scheme 2).

The molecular structure of **2a** was unambiguously determined by single-crystal X-ray diffraction, which is shown in Figure 1 together with the atom-labeling scheme. Selected bond distances and angles are listed in Table 1.

The bond distances C(1)–O(1) and C(2)–O(2) are 1.352(7) and 1.329(7) Å, respectively, showing their single-bond character. Although the bond distance C(4)–C(5) is slightly short [1.35(1) Å], no significant bond alternation is found in the other C–C bond distances in the benzo ring [1.386(8)–1.427(8) Å]. Therefore, complex **2a** is best regarded as a divalent dioxaruthenacycle complex, rather than an alternative canonical form: the *ortho*-quinone structure in Ru(0) .¹⁹

The $^3\text{1P}\{^1\text{H}\}$ NMR spectrum of **2a**, as expected, shows an A_2X_2 spin system at δ 11.9 and 1.7, suggesting the presence of a dioxaruthenacycle ring in an octahedral geometry. In the ^1H NMR spectrum, the characteristic methoxy resonance disappeared. These spectroscopic features in a solution state are

consistent with the X-ray structure of **2a**. The C–O bond cleavage reaction of 2-methoxyphenol was also confirmed by protonolysis of **2a**, where exposure of **2a** in acetone- d_6 to dry HCl gas evolved catechol in 97% yield (eq 1).



Complex **2a** showed poor reactivity toward hydrogenolysis, but **2a** gave catechol and $\text{cis-RuH}_2(\text{PMe}_3)_4$ in 33% and 32% yields, respectively, by the reaction with H_2 (6.8 MPa) at 70 °C for 20 h.

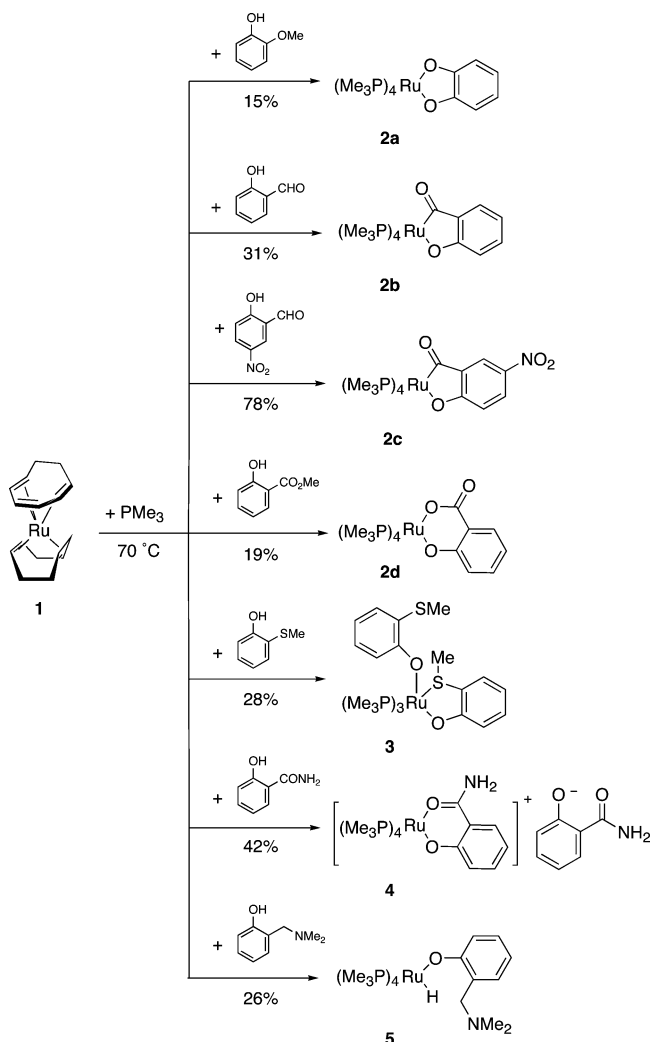
Similar treatments of **1**/ PMe_3 with salicylaldehyde, 5-nitrosalicylaldehyde, and methyl salicylate also produced corresponding oxaruthenacycle complexes $\text{cis-Ru}[\text{OC}_6\text{H}_4(\text{CO}-2)-\kappa^2\text{O},\text{C}](\text{PMe}_3)_4$ (**2b**), $\text{cis-Ru}[\text{OC}_6\text{H}_3(\text{CO}-2)(\text{NO}_2-4)-\kappa^2\text{O},\text{C}](\text{PMe}_3)_4$ (**2c**), and $\text{cis-Ru}[\text{OC}_6\text{H}_4(\text{CO}_2-2)-\kappa^2\text{O},\text{O}'](\text{PMe}_3)_4$ (**2d**) in 31%, 78%, and 19% yields, respectively, by the C–H or C–O bond cleavage reactions of the *ortho* substituent group. Among these complexes, single crystals suitable for X-ray analysis were obtained for **2c**, and the molecular structure is depicted in Figure 1, showing formation of a five-membered oxaruthenacycle complex.²⁰ One of the structural features of **2c** is that the bond distance $\text{Ru}(1)\text{--P}(2)$ [2.411(2) Å] is significantly longer than their covalent radii (2.34 Å).²¹ For compensation of this phenomenon, $\text{Ru}(1)\text{--C}(7)$ [1.992(2) Å] is slightly shorter than their covalent radii (2.01 Å). Therefore, C(7) has a strong *trans* influence probably due to the presence of p_π electrons in C(7).

(19) Formation of *p*-quinone complexes are recently reported: (a) Ura, Y.; Sato, Y.; Shiotsuki, M.; Suzuki, T.; Wada, K.; Kondo, T.; Mitsudo, T. *Organometallics* **2003**, 22, 77. (b) Mitsudo, T.; Ura, Y.; Kondo, T. *J. Organomet. Chem.* **2004**, 689, 4530.

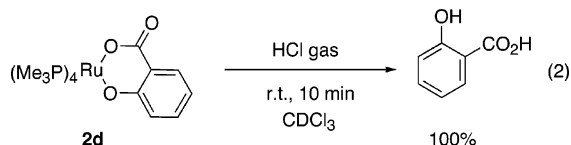
(20) For X-ray analysis of **2c**, two crystallographically independent molecules were found in a unit cell. Since they were isomorphous and their bond distances and angles were basically comparable to each other, the molecular structure of one of them was shown in Figure 1.

(21) Emsley, J. *The Elements*, 2nd ed., Oxford Univ., Oxford, 1991.

Scheme 2



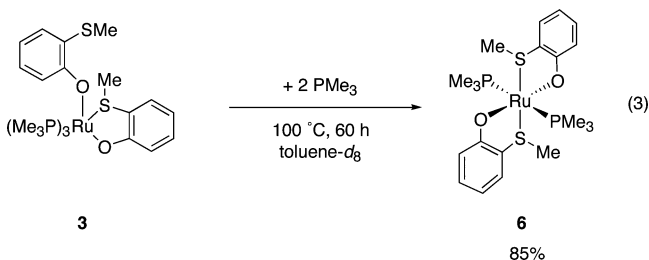
Complexes **2b–d** were also characterized by NMR and elemental analyses. As a typical example, characterization of **2d** is noteworthy. In the ^1H NMR spectrum of **2d**, the methyl resonance around the ester region disappeared. The $^{31}\text{P}\{^1\text{H}\}$ NMR spectrum of **2d** shows an AMX_2 pattern at δ 16.3, 12.0, and 1.31 in CDCl_3 , whereas these resonances are completely different from those for **2b** (see Experimental Section), suggesting that not the $\text{C}(\text{O})\text{--}\text{OMe}$ bond but the $\text{C}(\text{O})\text{O--Me}$ bond is cleaved to yield a six-membered oxaruthenacycle. The elemental analysis of **2d** also supports formation of the six-membered oxaruthenacycle. Consistently, the structure of **2d** was also confirmed by the chemical reaction, where exposure of **2d** in chloroform- d_1 to dry HCl gas at room temperature for 10 min liberated salicylic acid in quantitative yield (eq 2).



Contrary to these facts, reaction of **1**/ PMe_3 with 2-hydroxythioanisole at 70°C for 5 days was found to give the diaryloxoruthenium(II) complex *fac*- $\text{Ru}[\text{OC}_6\text{H}_4(\text{SMe-2})\text{-}\kappa^2\text{O},\text{S}][\text{OC}_6\text{H}_4(\text{SMe-2})\text{-}\kappa^1\text{O}](\text{PMe}_3)_3$ (**3**), which was characterized by NMR, X-ray analysis, and the elemental analysis. The molecular structure of **3** is depicted in Figure 2 together with the atom-

labeling scheme, and the bond distances and angles are listed in Table 2.

The molecular structure of **3** indicates formation of a five-membered ruthenacycle ring, but the C–S bond in the aryloxo moieties remains attached. The bond distances between the chelated and nonchelated aryloxo fragments are almost comparable, but the bond angle $\text{Ru}(1)\text{--}\text{O}(1)\text{--}\text{C}(1)$ [$118.6(6)^\circ$] is significantly smaller than $\text{Ru}(1)\text{--}\text{O}(2)\text{--}\text{C}(8)$ [$136.8(6)^\circ$], indicating restriction due to formation of a five-membered ring. Since bond distances $\text{Ru}(1)\text{--}\text{P}(1)$ [$2.243(2)\text{ \AA}$] and $\text{Ru}(1)\text{--}\text{P}(2)$ [$2.237(2)\text{ \AA}$] are also comparable, there seems to be little difference in the *trans* influence of $\text{O}(1)$ and $\text{O}(2)$. The $^{31}\text{P}\{^1\text{H}\}$ NMR data show an AMN pattern at δ 17.4, 15.4, and 14.0. The coordinated and uncoordinated SMe groups resonate at δ 2.29 (d) and 2.19 (s), respectively, suggesting rigid coordination of the SMe group in solution. Since compound **3** was a potential intermediate for a C–S bond cleavage reaction, further treatment of **3** was performed. However, attempting to heat **3** at 100°C in toluene- d_8 in the presence of PMe_3 resulted in the liberation of a PMe_3 ligand and coordination of the second SMe group to form *trans*- $\text{Ru}[\text{OC}_6\text{H}_4(\text{SMe-2})\text{-}\kappa^2\text{O},\text{S}](\text{PMe}_3)_2$ (**6**) in 85% yield (eq 3), and no C–S bond cleavage product was observed at all.



Treatment of **1**/ PMe_3 with 2-hydroxybenzamide and 2-*N,N*-dimethylaminomethylphenol gave *cis*- $[\text{Ru}\{\text{OC}_6\text{H}_4(\text{CONH}_2\text{-2})\text{-}\kappa^2\text{O},\text{O}'\}(\text{PMe}_3)_4]^+[\text{OC}_6\text{H}_4(\text{CONH}_2\text{-2})]^-$ (**4**) and *cis*- $\text{RuH}[\text{OC}_6\text{H}_4(\text{CH}_2\text{NMe}_2\text{-2})](\text{PMe}_3)_4$ (**5**) in 42% and 26% yields, respectively. Neither C–N nor N–H bond cleavage reaction took place for these substrates.

2,6-Disubstituted Phenols. Reactions of this system with a series of 2,6-disubstituted phenols were performed. As expected, treatment of **1**/ PMe_3 with 2,6-dimethoxyphenol in benzene at 70°C for 10 days followed by workup procedure yielded yellow needles of the oxaruthenacycle complex *cis*- $\text{Ru}[\text{OC}_6\text{H}_3(\text{O-2})(\text{OMe-6})\text{-}\kappa^2\text{O},\text{O}'](\text{PMe}_3)_4$ (**2e**) in 11% yield. It is worthwhile to note that this C–O bond cleavage reaction is expected to proceed via an aryloxoruthenium intermediate, where the chalcogen anchor brings the proximate C–O bond to the ruthenium center, leading to the bond cleavage reaction. Therefore, unsymmetrically 2,6-disubstituted phenols are regarded as good probes for chemoselectivity in the carbon–heteroatom bond cleavage reaction (Chart 1).

Although we have reported facile sp^3 C–H bond cleavage reaction of 2,6-xylenol and 2,6-dimethylbenzenethiol by the **1**/ PMe_3 system,^{15,16} the C–O bond in the methoxy group was cleaved and the methyl group remained as a spectator group to form **2f** when 2-methoxy-6-methylphenol was employed as a substrate (Scheme 3). The C–O bond in the ester group showed higher reactivity than the methyl or methoxy group (compounds **2g** and **2h**). The C–H bond in the formyl group was also easily cleaved (compounds **2i** and **2j**). Among complexes **2e–j**, single crystals of **2g**, **2h**, and **2j** suitable for X-ray diffraction studies were obtained, and their molecular structures are shown in Figure 3 and selected bond distances and angles are tabulated

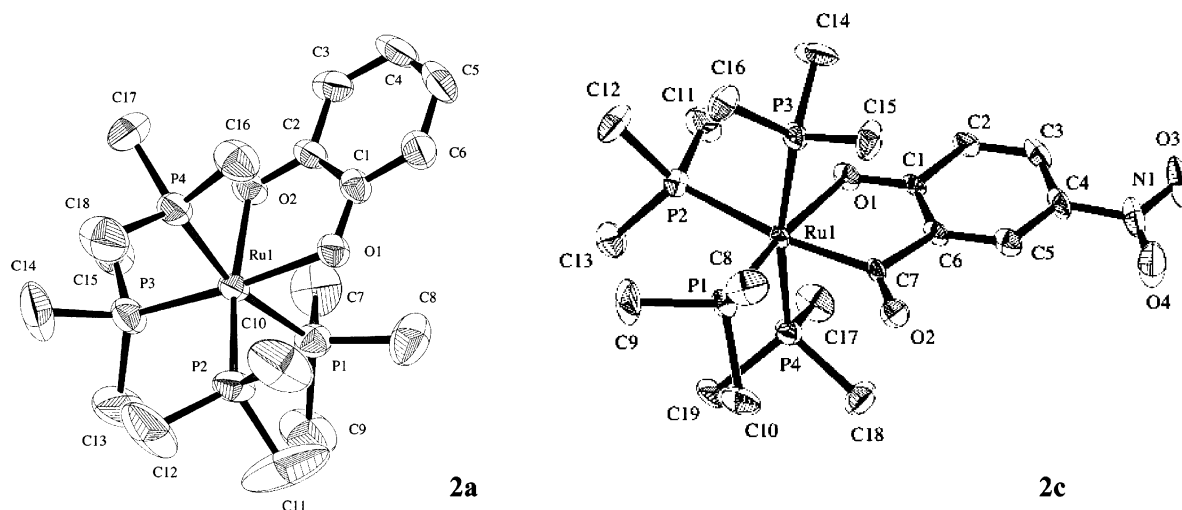


Figure 1. Molecular structures of *cis*-Ru[OC₆H₄(O-2)- κ^2 O,O'](PMe₃)₄ (**2a**) and *cis*-Ru[OC₆H₃(CO-2)(NO₂-4)- κ^2 O,C](PMe₃)₄ (**2c**). All hydrogen atoms are omitted for clarity. Ellipsoids represent 50% probability.

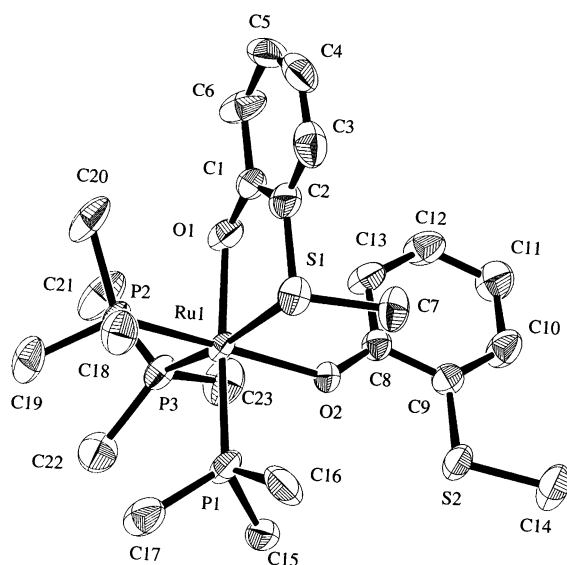
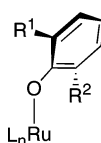


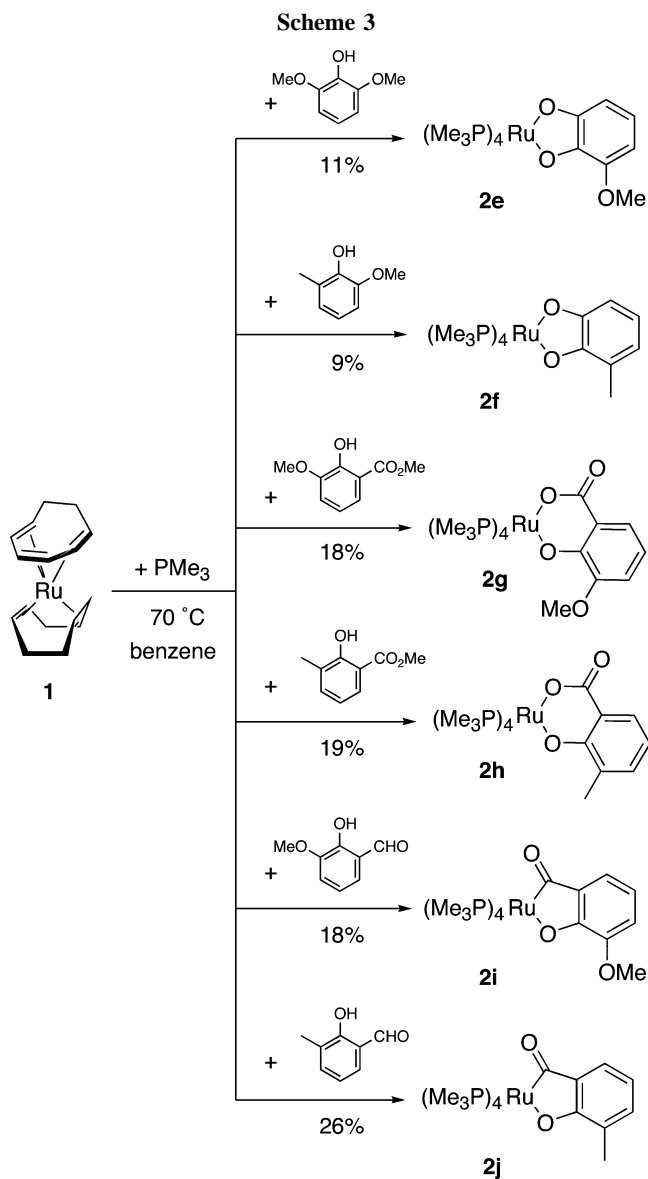
Figure 2. Molecular structure of complex **3**. All hydrogen atoms are omitted for clarity. Ellipsoids represent 50% probability.

Chart 1



in Table 3. It is notable that these chemoselective reactions proceeded exclusively, although yields of the oxaruthenacycle complexes are moderate based on the NMR studies (50–83%).

By taking into account the results employing asymmetric 2,6-disubstituted phenols, we can conclude that the ruthenium complex has a tendency to cleave the carbon–heteroatom bond in the following order: formyl C–H bond in ArC(O)–H, ester C–O bond in ArC(O)O–Me > ether C–O bond in ArO–Me > methyl C–H bond in ArCH₂–H as shown in Chart 2. The reported bond dissociation energies (BDEs) for the related bonds in present study are summarized in Table 4. Interestingly, although the strength of the formyl C–H bond of benzaldehyde is comparable to that of the methyl C–H bond of toluene, the competitive reaction by use of 2-formyl-6-methylphenol demonstrates exclusive cleavage of the formyl C–H bond. Moreover, whereas PhCH₂–NMe₂ and PhS–Me have relatively low



BDEs, neither the C–N nor C–S bond in 2-dimethylamino-methylphenol and 2-hydroxythioanisole could be cleaved under these conditions. Thus, the BDE is not responsible for the trend.

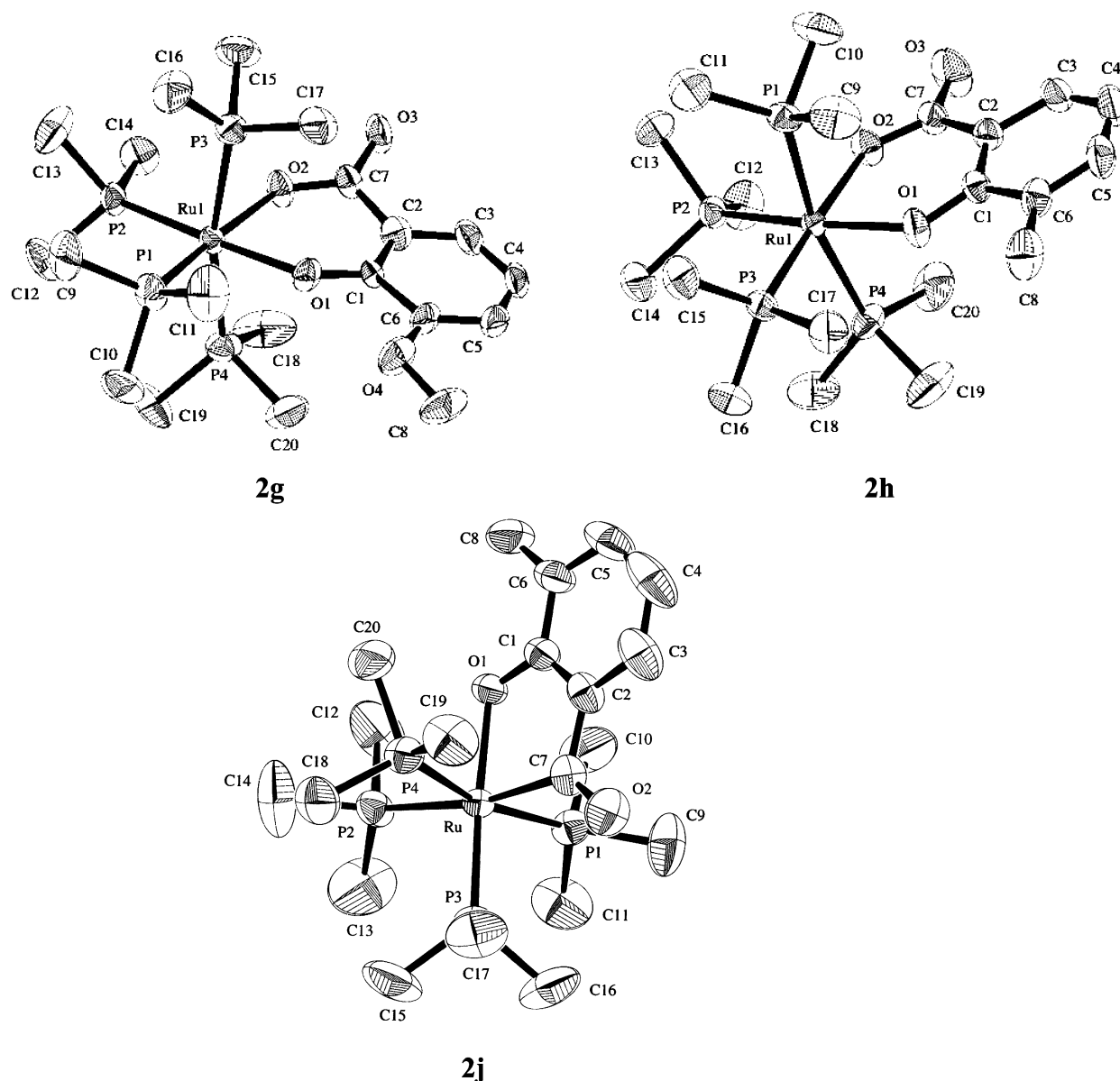


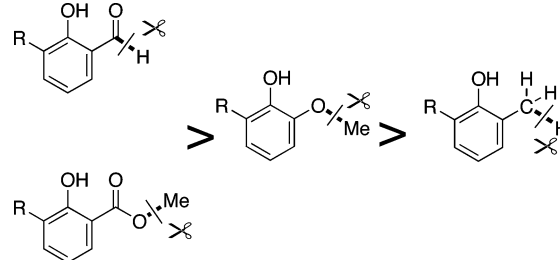
Figure 3. Molecular structures of *cis*-Ru[OC₆H₃(CO₂-2)(OMe-6)- κ^2 O,O'](PMe₃)₄ (**2g**), *cis*-Ru[OC₆H₃(CO₂-2)(Me-6)- κ^2 O,C](PMe₃)₄ (**2h**), and *cis*-Ru[OC₆H₃(CO-2)(Me-6)- κ^2 O,C](PMe₃)₄ (**2j**). All hydrogen atoms are omitted for clarity. Ellipsoids represent 50% probability.

On the other hand, the relative bond strengths in the ruthenium–heteroatom bond are reported as follows: Ru–H > Ru–OAr > Ru–NHPh > Ru–CH₂Ph in (Me₃P)₄HRu–X²² and Ru–C(sp) > Ru–O > Ru–H > Ru–C(sp³) > Ru–N in Cp*(Me₃P)₂Ru–X.²³ Thus, the stability of the resulting Ru–X bond could be responsible for the selectivity in these bond cleavages, although further detailed analyses are required to prove this.

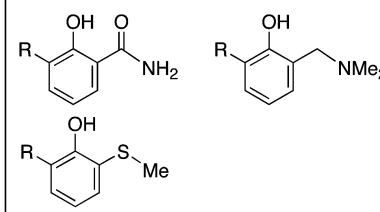
Mechanistic Studies. In order to shed lights on the reaction mechanism, time-course curves monitored by NMR for the reaction of **1**/PMe₃ with methyl salicylate in benzene-*d*₆ at 70 °C were analyzed, as shown in Figure 4.

Immediately after addition of PMe₃ to a benzene-*d*₆ solution of **1**, a monophosphine complex, Ru(η^4 -1,5-COD)(η^4 -1,3,5-COT)(PMe₃) (**7**), was dominantly formed. Then, *fac*-Ru(6- η^1 :1-3- η^3 -C₈H₁₀)(PMe₃)₃ (**8**), *fac*-Ru(6- η^1 :1-3- η^3 -C₈H₁₂)(PMe₃)₃ (**9**), and Ru(η^4 -1,5-COD)(PMe₃)₃ (**10**) were produced. Although

Chart 2



inactive toward carbon–heteroatom or N–H bond



(22) Hartwig, J. F.; Andersen, R. A.; Bergman, R. G. *Organometallics* **1991**, *10*, 1875.

(23) Bryndza, H. E.; Fong, L. K.; Paciello, R. A.; Tam, W.; Bercaw, J. E. *J. Am. Chem. Soc.* **1987**, *109*, 1444.

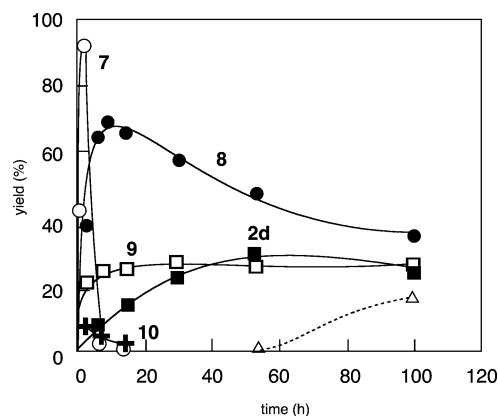


Figure 4. Time-course curves for the reaction of $\text{Ru}(\eta^4\text{-1,5-COD})\text{-(}\eta^6\text{-1,3,5-COT)}\text{-(1)}/\text{PMe}_3$ at 70 °C in benzene- d_6 . open circles: $\text{Ru}(\eta^4\text{-1,5-COD})(\eta^4\text{-1,3,5-COT})(\text{PMe}_3)_3$ (**7**). closed circles: $\text{fac-Ru}(6\text{-}\eta^1\text{-1-3-}\eta^3\text{-C}_8\text{H}_{10})(\text{PMe}_3)_3$ (**8**). open squares: $\text{fac-Ru}(6\text{-}\eta^1\text{-1-3-}\eta^3\text{-C}_8\text{H}_{12})(\text{PMe}_3)_3$ (**9**). closed squares: $\text{cis-Ru}[\text{OC}_6\text{H}_4(\text{CO}_2\text{-2-}\kappa^2\text{O},\text{O}')](\text{PMe}_3)_4$ (**2d**). crosses: $\text{Ru}(\eta^4\text{-1,5-COD})(\text{PMe}_3)_3$ (**10**). open triangles: unknown species.

complexes **7**,²⁴ **8**,²⁴ and **10**²⁵ are documented, complex **9** was a new species. Thus **9** was prepared and characterized by independent reaction. The molecular structure of **9** is depicted in Figure 8.

It is worthwhile to note that the C–O bond cleavage product **2d** seems to be formed with a decrease of **8**. In fact, complex **2d** was cleanly formed when isolated **8** was employed as the starting compound in benzene- d_6 (Figure 5a). It is notable that not a zerovalent but a divalent ruthenium species **8** plays dominant role in these carbon–heteroatom bond cleavage reactions.

When the reaction of **8** with methyl salicylate was performed in a polar solvent, DMSO- d_6 (DMSO = dimethylsulfoxide ($\text{C}_2\text{H}_6\text{OS}$)), the cationic cyclooctadienyl complex $[\text{Ru}(\eta^5\text{-C}_8\text{H}_{11})(\text{PMe}_3)_3]^+[\text{OC}_6\text{H}_4(\text{CO}_2\text{Me-2})]^-$ (**11**) was formed as a dominant product at the initial stage (Figure 5b). This complex is probably produced by protonation of the C_8H_{10} ligand in **8** as reported previously.^{15b} Figure 5b shows a typical successive reaction profile, where **11** is regarded as an intermediate for the C–O bond cleavage of methyl salicylate. While complex **11** was not detected in benzene- d_6 , it is observed in DMSO- d_6 probably due to stabilization of the cationic complex in a polar medium. It is also notable that the rate for the formation of **2d** in DMSO- d_6 was almost comparable to that in benzene- d_6 , suggesting a nonpolar transition state for the C–O bond cleavage reaction.

As shown in Figure 6a, the rate for the formation of the oxaruthenacycle complex was not affected by the amount of added methyl salicylate and PMe_3 , suggesting the process took place without liberation of the PMe_3 ligand. Either an electron-donating or -withdrawing substituent in methyl salicylate also did not affect the C–O bond cleavage reaction (Figure 6b).

The rate for the C–O bond cleavage reaction of isopropyl salicylate was significantly slower than that of methyl salicylate (Figure 7).

The fate of the methyl group in methyl salicylate is also surveyed. Treatment of **8** with twice the amount of methyl salicylate in the presence of 8 equiv of PMe_3 in DMSO- d_6 at

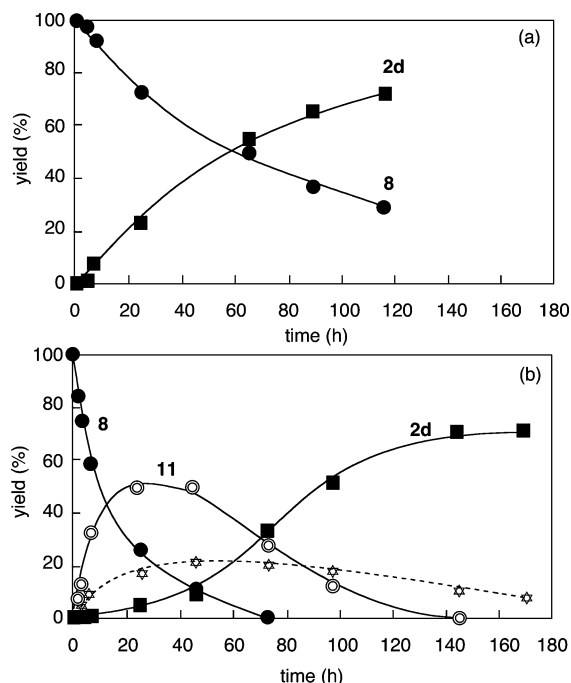


Figure 5. Time-course curves for the reaction of $\text{fac-Ru}(6\text{-}\eta^1\text{-1-3-}\eta^3\text{-C}_8\text{H}_{10})(\text{PMe}_3)_3$ (**8**) with methyl salicylate in the presence of PMe_3 at 70 °C in C_6D_6 (a) or in DMSO- d_6 (b). closed circles: of $\text{fac-Ru}(6\text{-}\eta^1\text{-1-3-}\eta^3\text{-C}_8\text{H}_{10})(\text{PMe}_3)_3$ (**8**). closed squares: $\text{cis-Ru}[\text{OC}_6\text{H}_4(\text{CO}_2\text{-2-}\kappa^2\text{O},\text{O}')](\text{PMe}_3)_4$ (**2d**). double circles: $[\text{Ru}(\eta^5\text{-C}_8\text{H}_{11})(\text{PMe}_3)_3]^+[\text{OC}_6\text{H}_4(\text{CO}_2\text{Me-2})]^-$ (**11**). stars: unidentified tetraphosphine complex.

70 °C for 4 days in a sealed NMR tube resulted in the formation of the C–O bond cleavage product **2d** in 76% yield with concomitant formation of methyl 2-methoxybenzoate (50%) (Scheme 4). In this process, although evolution of hydrogen gas was detected by GLC with formation of 1,3-COD (13%), 1,4-COD (7%), 1,3,5-COT (4%), and 1,5-COD (3%), methane was not detected by GLC analysis of the gas phase. 5-Methyl-1,3-cyclooctadiene,²⁶ which is a putative methylated product of the cyclooctadienyl ligand, was not formed. Similar treatment of **8** with 2,6-dimethoxyphenol gave **2e** (56%) and 1,2,3-trimethoxybenzene (46%). The GLC analysis of the gas phase showed evolution of hydrogen and a trace amount of methane. These experiments clearly show that the cleaved methyl group in the ester or ether was mainly trapped by aryloxides.

By taking into account these experimental data, a possible mechanism has been proposed for the C–O bond cleavage reaction of methyl salicylate as a typical example. First of all, treatment of **1** with PMe_3 gives **8**, which is protonated by the first methyl salicylate, giving the cationic cyclooctadienyl complex **11** (Scheme 5).

Although we cannot detect any intermediate for the C–O bond cleavage during the course of the reaction, a divalent diaryloxo complex (**A**) is the most probable intermediate. The most probable transition state for the C–O bond cleavage reaction is a concerted transition state **B**, since the reaction is not affected by the addition of PMe_3 and methyl salicylate as well as solvent polarity change, but is greatly retarded when a bulky ester is employed. Finally, the ruthenacycle complex **2d** is produced with concomitant formation of methyl 2-methoxybenzoate.

For further investigation of the C–O bond cleavage process, $\text{trans-RuCl}_2(\text{PMe}_3)_4$ (**12**) was treated with 3.8 equiv of potassium

(24) (a) Hirano, M.; Marumo, T.; Miyasaka, T.; Fukuoka, A.; Komiya, S. *Chem. Lett.* **1997**, 297. (b) Komiya, S.; Planas, J. G.; Onuki, K.; Lu, Z.; Hirano, M. *Organometallics* **2000**, 19, 4051. (c) Hirano, M.; Asakawa, R.; Nagata, C.; Miyasaka, T.; Komine, N.; Komiya, S. *Organometallics* **2003**, 22, 2378.

(25) Bennett, M. A.; Lu, Z.; Wang, X.; Bown, M.; Hockless, D. C. R. *J. Am. Chem. Soc.* **1998**, 120, 10409.

(26) Pearson, A. J.; Balasubramanian, S.; Srinivasan, K. *Tetrahedron* **1993**, 49, 5663.

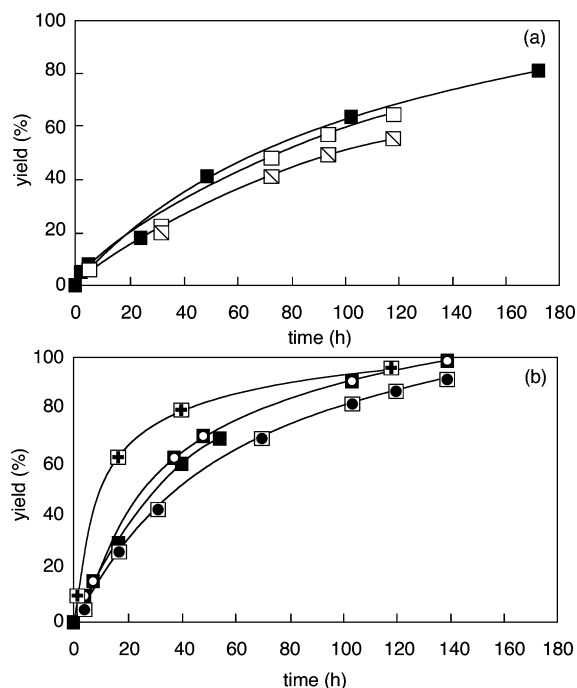


Figure 6. (a) Effect on added PMe_3 and methyl salicylate for the yield of $\text{cis-Ru}[\text{OC}_6\text{H}_4(\text{CO}_2\text{-}2)\text{-}\kappa^2\text{O},\text{O}'](\text{PMe}_3)_4$ (**2d**) starting from **8** in benzene- d_6 at 70 °C. open squares: methyl salicylate (2.7 equiv/**8**), PMe_3 (9.0 equiv/**8**). closed squares: methyl salicylate (9.0 equiv/**8**), PMe_3 (9.0 equiv/**8**). open squares with diagonal line: methyl salicylate (2.7 equiv/**8**), PMe_3 (1.7 equiv/**8**). (b) Effect on substituents in methyl salicylate for the yield of oxaruthenacycle complexes starting from **8** in benzene- d_6 at 70 °C. open squares with cross: methyl 5-fluorosali-cylate. closed squares with an open circle: methyl 5-methoxysali-cylate. closed squares: methyl sali-cylate. open squares with a closed circle: methyl 4-methoxysali-cylate.

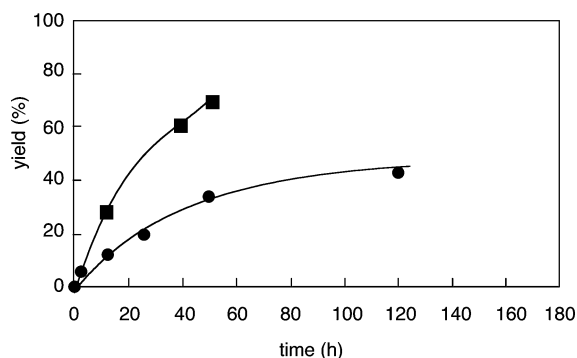


Figure 7. Time-yield curves for the formation of $\text{cis-Ru}[\text{OC}_6\text{H}_4(\text{CO}_2\text{-}2)\text{-}\kappa^2\text{O},\text{O}'](\text{PMe}_3)_4$ (**2d**) by the reaction of $\text{fac-Ru}(6\text{-}\eta^1\text{-}1\text{-}3\text{-}\eta^3\text{-}\text{C}_8\text{H}_{10})(\text{PMe}_3)_3$ (**8**) with methyl salicylate (closed squares) or isopropyl salicylate (closed circles) in the presence of PMe_3 at 70 °C in C_6D_6 .

salt of methyl salicylate in refluxing THF (THF = tetrahydrofuran ($\text{C}_4\text{H}_8\text{O}$)) for 4 days, and as expected, the product after workup was identified as the corresponding ruthenacycle **2d** in 65% yield. Similarly, treatment of **12** with potassium 2,6-dimethoxyphenoxide also produced **2e** in 61% yield. However, in these metathetical reactions starting from **12**, methyl 2-methoxysali-cylate and 1,2,3-trimethoxybenzene were produced only in 7% yields in both cases. Further investigation of the reaction of **12** with 3.1 equiv of potassium salt of methyl salicylate in DME (DME = 1,2-dimethoxyethane ($\text{C}_4\text{H}_{10}\text{O}_2$)) at 70 °C for 3 days revealed formation of **2d** (10%) and an unidentified new species (68%) having an ABX pattern in the $^{31}\text{P}\{^1\text{H}\}$ NMR

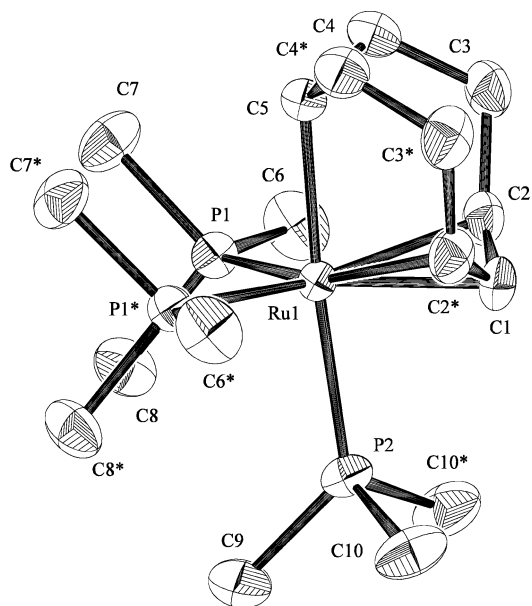
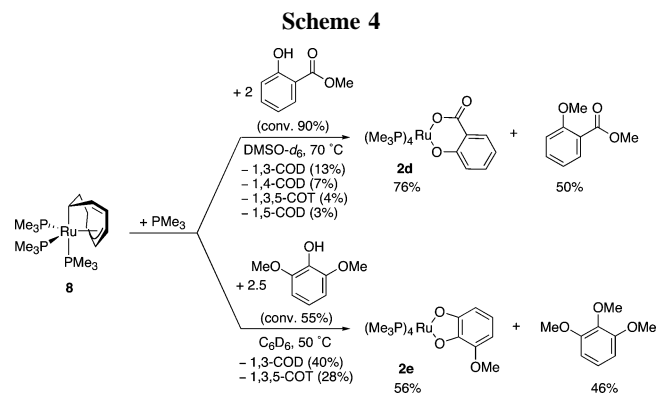
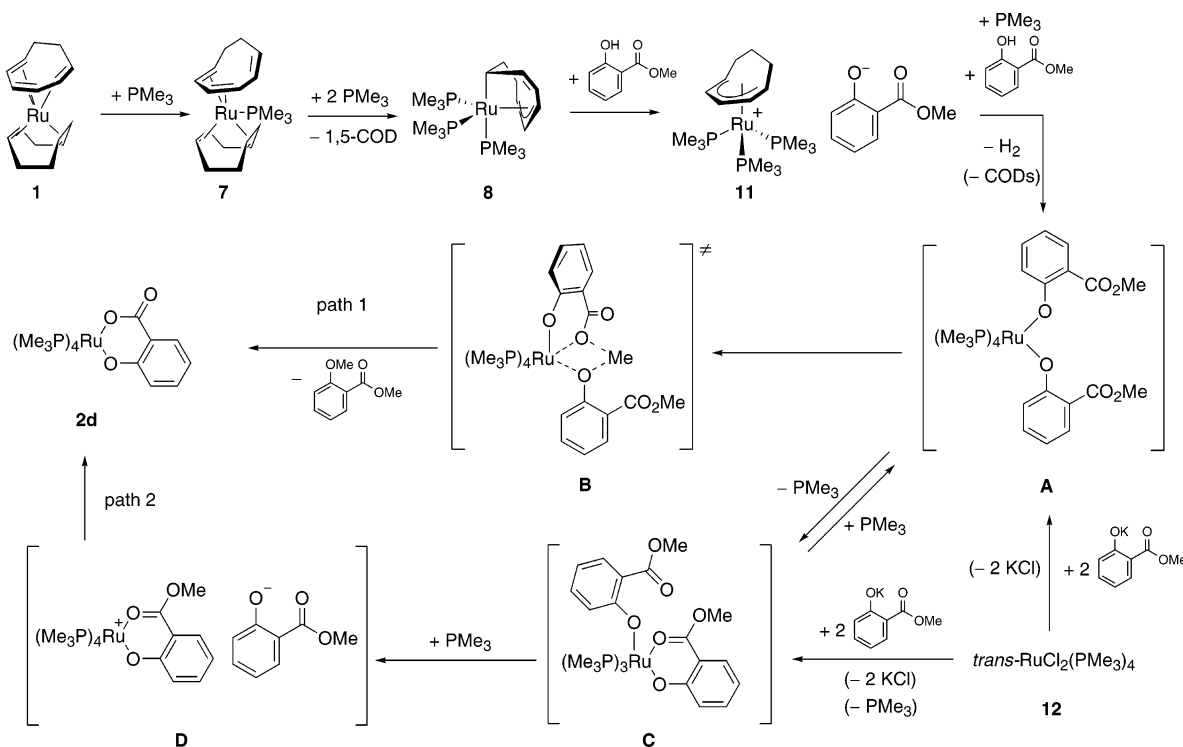


Figure 8. Molecular structure of $\text{fac-Ru}(6\text{-}\eta^1\text{-}1\text{-}3\text{-}\eta^3\text{-}\text{C}_8\text{H}_{12})(\text{PMe}_3)_3$ (**9**). All hydrogen atoms are omitted for clarity. Ellipsoids represent 50% probability. The molecule has C_s symmetry, and atoms designated with asterisk were generated by the symmetrical operation.



spectrum at δ 30.5 (dd, $J = 44, 39$ Hz), 27.0 (dd, $J = 44, 39$ Hz), and 22.6 (t, $J = 39$ Hz). These three phosphorus atoms are magnetically inequivalent, and they are close to those for a diaryloxoruthenium(II) complex, $\text{fac-Ru}[\text{OC}_6\text{H}_4(\text{SMe-}2)\text{-}\kappa^2\text{O},\text{S}][\text{OC}_6\text{H}_4(\text{SMe-}2)\text{-}\kappa^1\text{O}](\text{PMe}_3)_3$ (**3**), suggesting formation of intermediate **C** in Scheme 5. Immediately after addition of 1 equiv of PMe_3 to the mixture, this species disappeared and a new AMX_2 species (54%) appeared at δ 19.9 (q, $J = 34$ Hz, 1P), 12.4 (q, $J = 34$ Hz, 1P), and -1.43 (t, $J = 34$ Hz, 2P) in the $^{31}\text{P}\{^1\text{H}\}$ NMR spectrum with concomitant formation of **2d** in 16% yield. Since the resonances for the new species having an AMX_2 spin system are close to those for the cationic aryloxo complex $\text{cis-Ru}\{\text{OC}_6\text{H}_4(\text{CONH}_2\text{-}2)\text{-}\kappa^2\text{O},\text{O}'\}(\text{PMe}_3)_4^+[\text{OC}_6\text{H}_4(\text{CONH}_2\text{-}2)]^-$ (**4**), we tentatively assigned this species as intermediate **D** in Scheme 5. Heating of this species at 70 °C for 30 min gave a mixture of the C–O bond cleavage product **2d** (76%) and **D** (16%). It is notable that methyl 2-methoxybenzoate was not observed, and the fate of the cleaved methyl group in the ester group could not be clarified in this process. By taking into account these facts, there may be at least two independent processes giving **2d** (paths 1 and 2 in Scheme 5). However, these data suggest that intermediate **C** could be produced only when a PMe_3 was lost during the reaction, and path 1 would be the dominant process starting from **1**.

Scheme 5



Concluding Remarks. The carbon–heteroatom bonds in the ester or ether group at the *ortho* position of aryloxo are easily cleaved in divalent ruthenium complexes. Several observations are consistent with a bond cleavage reaction by a concerted mechanism involving coordinatively saturated diaryloxoruthenium(II) intermediates. This concerted bond cleavage reaction is also proposed for ruthenium(II) complexes such as *cis*- $\text{Ru}(\text{OC}_6\text{H}_4\text{Me-4})_2(\text{PMe}_3)_4$ ²⁸ and *cis*- $\text{Ru}[\text{OC}(\text{O})\text{C}(\text{Me})=\text{CH}_2]_2(\text{PMe}_3)_4$.¹⁸ The present 2,6-disubstituted aryloxo system also provides a good probe to seek the trend of carbon–heteroatom bond cleavage reactions. The most relevant is the observation that the cleaved methyl group in methyl ester (and also methyl ether) is trapped by the OAr group, giving an anisole derivative. We believe this work provides important information for the bond cleavage reactions in divalent ruthenium complexes.

Experimental Section

All manipulations and reactions were performed under dry nitrogen with the use of standard Schlenk and vacuum line techniques. Toluene, benzene, hexane, THF, DME, and Et_2O were distilled over sodium benzophenone ketyl, pentane was distilled over potassium benzophenone ketyl, and CH_2Cl_2 and acetonitrile were distilled from Drierite. Ethanol was dried over calcium chloride and distilled under nitrogen over magnesium ethoxide; these solvents were stored under nitrogen. $\text{Ru}(\eta^4\text{-1,5-COD})(\eta^6\text{-1,3,5-COT})$ (**1**)²⁹ was prepared according to literature procedures, but magnetic stirring was used instead of sonication. $\text{Ru}(\eta^4\text{-1,5-COD})(\eta^4\text{-1,3,5-COT})(\text{PMe}_3)$ (**7**)²⁴, *fac*- $\text{Ru}(\eta^6\text{-1:1-3-}\eta^3\text{-C}_8\text{H}_{10})(\text{PMe}_3)_3$ (**8**)^{24a}, $\text{Ru}(\eta^4\text{-1,5-COD})(\text{PMe}_3)_3$ (**10**)²⁵ and *trans*- $\text{RuCl}_2(\text{PMe}_3)_4$ (**12**)³⁰ were characterized according to the reported literature.

(27) Luo, Y.-R. in *Handbook of Bond Dissociation Energies in Organic Compounds*, CRC (Boca Raton) 2003.

(28) Hartwig, J. F.; Bergman, R. G.; Andersen, R. A. *J. Organomet. Chem.* **1990**, 394, 417.

(29) Itoh, K.; Nagashima, H.; Ohshima, T.; Oshima, N.; Nishiyama, H. *J. Organomet. Chem.* **1984**, 272, 179.

(30) Jones, R. A.; Real F. R.; Wilkinson, G.; Galas, A. M. R.; Hursthouse, M. B.; Abdul Malik, K. M. *J. Chem. Soc., Dalton Trans.* **1980**, 511.

Trimethylphosphine was prepared by the treatment of $\text{P}(\text{O}^i\text{Pr})_3$ with methyl Grignard reagent.³¹ 2-*N,N*-Dimethylaminomethylphenol and methyl 3-methoxysalicylate were prepared according to literature methods.³² All other reagents were obtained from commercial suppliers (Wako Pure Chemical Ind., Aldrich, or TCI) and used as received. Chromatographic separation was carried out on Al_2O_3 (Merck, activity I, 250 mesh). GLC analyses were performed by a Shimadzu GC-14B equipped with a FID detector by use of a glass capillary column (TC-wax: 0.25 mm ϕ \times 30 m) or Shimadzu GC-3B equipped with a TCD detector by use of a glass packed column (molecular sieves or Polapack Q). The NMR spectra were recorded on a JEOL LA300 (^1H at 300.4 MHz). The internal reference was either tetramethylsilane or the residual solvent peak (CHCl_3 , CH_2Cl_2). CDCl_3 and CD_2Cl_2 were distilled over P_4O_{10} and stored under vacuum. Elemental analyses were performed on a Perkin-Elmer 2400 series II CHN analyzer.

***cis*- $\text{Ru}[\text{OC}_6\text{H}_4(\text{O-2})-\kappa^2\text{O},\text{O}'](\text{PMe}_3)_4$ (**2a**).** Complex **1** (101.9 mg, 0.3231 mmol) was placed in a Schlenk tube into which benzene (3.0 mL) was added under N_2 atmosphere. PMe_3 (130 μL , 1.26 mmol) and then 2-methoxyphenol (40.0 μL , 0.365 mmol) were added into the solution by a hypodermic syringe. The reaction mixture was heated at 70 $^\circ\text{C}$ for 6 days. All volatile matters were removed under reduced pressure, and the resulting yellow solid was recrystallized from cold toluene to give yellow needles of **2a** in 15% yield (15.0 mg, 0.048 mmol). Complexes **2b–j**, **3**, **4**, and **5** were also prepared by a similar procedure. ^1H NMR ($\text{CD}_3\text{-COCD}_3$): δ 1.26 (vt, $J = 3.2$ Hz, 18H, mutually *trans* PMe_3), 1.45 (m, 18H, PMe_3), 5.97 (dd, $J = 5.5, 3.7$ Hz, 2H, C_6H_4), 6.17 (dd, $J = 5.5, 3.7$ Hz, 2H, C_6H_4). $^{31}\text{P}\{^1\text{H}\}$ NMR (CD_3COCD_3): δ 1.7 (t, $J = 30$ Hz, 2P), 11.9 (t, $J = 30$ Hz, 2P). IR (KBr, cm^{-1}): 3047(w), 3031(w), 2993(w), 2970(w), 2909(w), 1559(m), 1474(m), 1420(w), 1299(w), 1255(m), 944(s), 720(m), 662(w). Anal. Calcd for $\text{C}_{18}\text{H}_{40}\text{O}_4\text{P}_4\text{Ru}$: C, 42.01; H, 7.85. Found: C, 42.15; H, 7.96.

(31) Kosolapoff, G. M.; Maier, L. In *Organic Phosphorus Compounds* Wiley, New York, 1972 and the procedure was referred to the following article: Burt, R. J.; Chatt, J.; Hussain, W.; Leigh, G. J. *J. Organomet. Chem.* **1979**, 182, 203.

(32) Cavitt, S. B.; Sarrafzadeh, R. H.; Gardner, P. D. *J. Org. Chem.* **1962**, 27, 1211.

Table 1. Selected Bond Distances (Å) and Angles (deg) for **2a** and **2c**

| 2a | | | |
|-----------------|-----------|-----------------|-----------|
| Ru(1)–P(1) | 2.388(2) | Ru(1)–P(2) | 2.273(2) |
| Ru(1)–P(3) | 2.273(2) | Ru(1)–P(4) | 2.372(2) |
| Ru(1)–O(1) | 2.112(4) | Ru(1)–O(2) | 2.130(4) |
| O(1)–C(1) | 1.352(7) | O(2)–C(2) | 1.329(7) |
| C(1)–C(2) | 1.427(8) | C(1)–C(6) | 1.386(8) |
| C(2)–C(3) | 1.393(8) | C(3)–C(4) | 1.405(10) |
| C(4)–C(5) | 1.35(1) | C(5)–C(6) | 1.40(1) |
| P(1)–Ru(1)–P(2) | 96.81(7) | P(1)–Ru(1)–P(3) | 94.04(7) |
| P(1)–Ru(1)–P(4) | 165.40(6) | P(1)–Ru(1)–O(1) | 84.6(1) |
| P(1)–Ru(1)–O(2) | 84.6(1) | O(1)–Ru(1)–O(2) | 80.0(1) |
| Ru(1)–O(1)–C(1) | 111.5(3) | Ru(1)–O(2)–C(2) | 110.6(3) |
| 2c | | | |
| Ru(1)–P(1) | 2.238(3) | Ru(1)–P(2) | 2.411(2) |
| Ru(1)–P(3) | 2.335(2) | Ru(1)–P(4) | 2.333(2) |
| Ru(1)–O(1) | 2.136(7) | Ru(1)–C(7) | 1.992(9) |
| O(1)–C(1) | 1.28(1) | O(2)–C(7) | 1.22(1) |
| O(3)–N(1) | 1.23(1) | O(4)–N(1) | 1.20(1) |
| N(1)–C(4) | 1.42(1) | C(1)–C(2) | 1.44(1) |
| C(1)–C(6) | 1.37(1) | C(2)–C(3) | 1.36(1) |
| C(3)–C(4) | 1.41(1) | C(4)–C(5) | 1.38(1) |
| C(5)–C(6) | 1.37(1) | C(6)–C(7) | 1.50(1) |
| P(1)–Ru(1)–P(2) | 101.0(1) | P(1)–Ru(1)–P(3) | 94.0(1) |
| P(1)–Ru(1)–P(4) | 94.7(1) | P(1)–Ru(1)–O(1) | 171.9(2) |
| P(1)–Ru(1)–C(7) | 90.2(3) | O(1)–Ru(1)–C(7) | 81.8(3) |
| Ru(1)–O(1)–C(1) | 110.5(5) | O(3)–N(1)–O(4) | 122(1) |
| Ru(1)–C(7)–O(2) | 133.3(6) | Ru(1)–C(7)–C(6) | 110.1(6) |
| O(2)–C(7)–C(6) | 116.5(8) | | |

cis-Ru[OC₆H₄(CO-2)- κ^2 O,C](PMe₃)₄ (2b**).** Treatment of **1** (123.0 mg, 0.3900 mmol) with PMe₃ (160.0 μ L, 1.546 mmol) and salicylaldehyde (50.0 μ L, 0.478 mmol) in benzene (5.0 mL) at 70 °C for 5 days followed by workup involving recrystallization from cold toluene gave pale yellow microcrystals of **2b** in 31% yield (47.0 mg, 0.121 mmol). This compound was characterized spectroscopically. ¹H NMR (C₆D₆): δ 0.96 (vt, J = 2.7 Hz, 18H, PMe₃), 1.07 (d, J = 5.4 Hz, 9H, PMe₃), 1.20 (d, J = 8.1 Hz, 9H, PMe₃), 6.68 (t, J = 7.2 Hz, 1H, C₆H₄), 7.22 (d, J = 8.1 Hz, 1H, C₆H₄), 7.31 (t, J = 7.4 Hz, 1H, C₆H₄), 8.06 (d, J = 8.3 Hz, 1H, C₆H₄). ³¹P{¹H} NMR (C₆D₆): δ -20.9 (t, J = 27 Hz, 1P), -5.6 (dd, J = 35, 26 Hz, 2P), 11.0 (t, J = 35 Hz, 1P). IR (KBr, cm⁻¹): 3035(w), 2969-(m), 2908(s), 1910(w), 1586(s), 1543(s), 1458(s), 1442(m), 1324-(s), 1302(m), 1232(w), 1126(m), 1082(w), 1014(w), 944(vs), 870(s), 758(m), 749(m), 713(s), 663(m), 630(m).

cis-Ru[OC₆H₃(CO-2)(NO₂-4)- κ^2 O,C](PMe₃)₄ (2c**).** Treatment of **1** (135.8 mg, 0.4305 mmol) with PMe₃ (140.0 μ L, 1.353 mmol) and 5-nitrosalicylaldehyde (149.2 mg, 0.8928 mmol) in THF (3.0 mL) at room temperature for 1 h followed by workup involving recrystallization from cold acetone gave red microcrystals of **2c** in 78% yield (192.5 mg, 0.3374 mmol). ¹H NMR (CD₂Cl₂): δ 1.12 (brs, 18H, PMe₃), 1.41 (m, 18H, PMe₃), 6.57 (d, J = 9.3 Hz, 1H, C₆H₃), 7.92 (d, J = 9.0 Hz, 1H, C₆H₃), 8.05 (d, J = 2.7 Hz, 1H, C₆H₃). ³¹P{¹H} NMR (CD₂Cl₂): δ -21.3 (td, J = 27, 5 Hz, 1P), -6.7 (dd, J = 27, 35 Hz, 2P), 12.6 (td, J = 35 Hz, 5H, 1P). IR (KBr, cm⁻¹): 2971(w), 2910(w), 1585(m), 1557(m), 1477(m), 1425(m), 1298(s), 1277(s), 938(s). Anal. Calcd for C₁₉H₃₉NO₄P₄Ru: C, 40.00; H, 6.89; N, 2.46. Found: C, 40.38; H, 7.06; N, 2.43.

cis-Ru[OC₆H₄(CO₂-2)- κ^2 O,C](PMe₃)₄ (2d**).** Treatment of **1** (242.1 mg, 0.767 mmol) with PMe₃ (400.0 μ L, 3.091 mmol) and methyl salicylate (120.0 μ L, 0.926 mmol) in benzene (3 mL) at 70 °C for 6 days followed by workup involving recrystallization from cold THF gave white microcrystals of **2d** in 19% yield (77.9 mg, 0.143 mmol). ¹H NMR (CDCl₃): δ 1.29 (vt, J = 3.1 Hz, 18H, PMe₃), 1.42 (d, J = 8.1 Hz, 18H, PMe₃), 6.33 (td, J = 7.6, 1.2 Hz, 1H, C₆H₄), 6.54 (d, J = 7.6 Hz, 1H, C₆H₄), 7.01 (td, J = 7.6, 1.8 Hz, 1H, C₆H₄), 8.14 (dd, J = 7.6, 1.8 Hz, 1H, C₆H₄). ³¹P{¹H} NMR (CDCl₃): δ 1.31 (t, J = 32 Hz, 2P), 12.0 (q, J = 32 Hz, 1P), 16.3 (q, J = 32 Hz, 1P). ¹³C{¹H} NMR (CDCl₃): δ 17.5 (t, J = 13 Hz, PMe₃), 20.97 (d, J = 28 Hz, PMe₃), 21.33 (d, J = 26 Hz, PMe₃),

Table 2. Selected Bond Distances (Å) and Angles (deg) for **3**

| | | | |
|-----------------|------------|-----------------|----------|
| Ru(1)–S(1) | 2.380(3) | Ru(1)–P(1) | 2.243(2) |
| Ru(1)–P(2) | 2.237(2) | Ru(1)–P(3) | 2.261(3) |
| Ru(1)–O(1) | 2.098(7) | Ru(1)–O(2) | 2.139(6) |
| S(1)–C(2) | 1.75(1) | S(1)–C(7) | 1.80(1) |
| S(2)–C(9) | 1.743(10) | S(2)–C(14) | 1.75(1) |
| O(1)–C(1) | 1.30(1) | O(2)–C(8) | 1.28(1) |
| C(1)–C(2) | 1.39(2) | C(1)–C(6) | 1.41(1) |
| C(2)–C(3) | 1.38(2) | C(3)–C(4) | 1.34(2) |
| C(4)–C(5) | 1.33(2) | C(5)–C(6) | 1.36(2) |
| C(8)–C(9) | 1.40(1) | C(8)–C(13) | 1.38(1) |
| C(9)–C(10) | 1.37(1) | C(10)–C(11) | 1.38(2) |
| C(11)–C(12) | 1.38(2) | C(12)–C(13) | 1.38(1) |
| S(1)–Ru(1)–P(1) | 96.3(1) | S(1)–Ru(1)–P(2) | 89.28(9) |
| S(1)–Ru(1)–P(3) | 167.91(10) | S(1)–Ru(1)–O(1) | 81.9(2) |
| S(1)–Ru(1)–O(2) | 86.0(2) | O(1)–Ru(1)–O(2) | 94.3(2) |
| Ru(1)–S(1)–C(2) | 97.8(4) | Ru(1)–S(1)–C(7) | 111.4(4) |
| C(2)–S(1)–C(7) | 100.2(5) | C(9)–S(2)–C(14) | 104.8(5) |
| Ru(1)–O(1)–C(1) | 118.6(6) | Ru(1)–O(2)–C(8) | 136.8(6) |

111.5 (s), 121.1 (s), 123.6 (d, J = 5.3 Hz), 131.0 (s), 134.3 (s), 170.5 (s), 171.4 (s). IR (KBr, cm⁻¹): 3035(w), 2908(s), 1910(w), 1586(s), 1543(s), 1458(s), 1442(m), 1302(m), 1277(m), 1232(w), 1126(m), 1082(w), 1014(w), 944(vs), 870(s), 758(m), 749(m), 713-(s), 663(m), 630(m). Anal. Calcd for C₁₉H₄₀O₃P₄Ru: C, 42.14; H, 7.45. Found: C, 42.09; H, 7.37.

cis-Ru[OC₆H₃(O-2)(OMe-6)- κ^2 O,O'](PMe₃)₄ (2e**).** Treatment of **1** (273.3 mg, 0.866 mmol) with PMe₃ (520.0 μ L, 3.516 mmol) and 2,6-dimethoxyphenol (137.8 mg, 0.894 mmol) in benzene (3 mL) at 70 °C for 10 days followed by workup involving crystallization from cold benzene gave yellow needles of **2e** in 11% yield (51.9 mg, 0.0953 mmol). ¹H NMR (C₆D₆): δ 1.01 (d, J = 7.8 Hz, 9H, PMe₃), 1.04 (d, J = 7.8 Hz, 9H, PMe₃), 1.09 (vt, J = 3.3 Hz, 18H, PMe₃), 4.09 (s, 3H, OMe), 6.66 (dd, J = 7.8, 1.6 Hz, 1H, C₆H₃), 6.75 (t, J = 7.8 Hz, 1H, C₆H₃), 6.92 (dd, J = 7.8, 1.6 Hz, 1H, C₆H₃). ³¹P{¹H} NMR (C₆D₆): δ 1.15 (t, J = 30 Hz, 2P), 11.20 (q, J = 30 Hz, 1P), 11.65 (q, J = 30 Hz, 1P). ¹³C{¹H} NMR (C₆D₆): δ 16.71 (t, J = 12 Hz, PMe₃), 22.26 (d, J = 23 Hz, PMe₃), 57.63 (s, OMe), 104.12 (s), 111.12 (s), 113.37 (s), 150.65 (s), 154.26 (d, J = 5 Hz), 166.43 (d, J = 5 Hz). Anal. Calcd for C₁₉H₄₂O₃P₄Ru: C, 41.99; H, 7.79. Found: C, 41.75; H, 7.86.

cis-Ru[OC₆H₃(O-2)(Me-6)- κ^2 O,O'](PMe₃)₄ (2f**).** Treatment of **1** (70.1 mg, 0.222 mmol) with PMe₃ (100.0 μ L, 0.9661 mmol) and 2-methoxy-6-methylphenol (35.4 mg, 0.256 mmol) in benzene (2.0 mL) at 70 °C for 8 days followed by workup involving recrystallization from cold acetone/hexane gave pale yellow microcrystals in 9% yield (10.4 mg, 0.00196 mmol). This compound was characterized spectroscopically. ¹H NMR (C₆D₆): δ 1.04 (m, 36H, PMe₃), 2.66 (s, 3H, Me), 6.83 (d, J = 7.0 Hz, 2H, C₆H₃), 7.05 (dd, J = 6.3, 2.5 Hz, 1H, C₆H₃). ³¹P{¹H} NMR (C₆D₆): δ 0.80 (q, J = 30 Hz, 2P), 10.6 (q, J = 30 Hz, 1P), 11.5 (q, J = 30 Hz, 1P).

cis-Ru[OC₆H₃(CO₂-2)(OMe-6)- κ^2 O,O'](PMe₃)₄ (2g**).** Treatment of **1** (132.7 mg, 0.4207 mmol) with PMe₃ (190.0 μ L, 1.836 mmol) and methyl 3-methoxysalicylate (77.2 mg, 0.424 mmol) in benzene (5.0 mL) at 70 °C for 5 days followed by workup involving recrystallization from cold acetone gave orange microcrystals of **2g** in 18% yield (42.5 mg, 0.0744 mmol). This compound was characterized spectroscopically. ¹H NMR (C₆D₆): δ 0.97 (d, J = 8.1 Hz, 9H, PMe₃), 1.01 (vt, J = 3.3 Hz, 18H, PMe₃), 1.03 (d, J = 8.4 Hz, 9H, PMe₃), 3.65 (s, OMe), 6.67 (t, J = 7.8 Hz, 1H, C₆H₃), 6.82 (dd, J = 7.2, 1.8 Hz, 1H, C₆H₃), 8.81 (dd, J = 8.3, 2.0 Hz, 1H, C₆H₃). ³¹P{¹H} NMR (C₆D₆): δ 0.9 (t, J = 32 Hz, 2P), 12.1 (q, J = 32 Hz, 1P), 15.6 (q, J = 32 Hz, 1P). IR (KBr, cm⁻¹): 3401(w), 3045(w), 2992(w), 2966(w), 2914(m), 2813(w), 13618(w), 1710(m), 1595(s), 1565(s), 1539(s), 1465(s), 1444(s), 1340(m), 1319(m), 1302(m), 1283(m), 1254(w), 1225(m), 1192(w), 1167(m), 1068(m), 1032(m), 979(sh), 944(vs), 862(m), 786(w), 757(w), 741(m), 717(m), 666(m), 617(w).

cis-Ru[OC₆H₃(CO₂-2)(Me-6)- κ^2 O,O'](PMe₃)₄ (2h**).** Treatment of **1** (114.9 mg, 0.3643 mmol) with PMe₃ (188.0 μ L, 1.816 mmol)

Table 3. Selected Bond Distances (Å) and Angles (deg) for **2g**, **2h**, and **2j**

| 2g | | | |
|-----------------|-----------|-----------------|-----------|
| Ru(1)–P(1) | 2.275(2) | Ru(1)–P(2) | 2.291(2) |
| Ru(1)–P(3) | 2.368(2) | Ru(1)–P(4) | 2.375(3) |
| Ru(1)–O(1) | 2.109(5) | Ru(1)–O(2) | 2.121(5) |
| O(1)–C(1) | 1.31(1) | O(2)–C(7) | 1.283(10) |
| O(3)–C(7) | 1.24(1) | O(4)–C(6) | 1.39(1) |
| O(4)–C(8) | 1.40(1) | C(1)–C(2) | 1.41(1) |
| C(1)–C(6) | 1.44(1) | C(2)–C(3) | 1.41(1) |
| C(2)–C(7) | 1.51(1) | C(3)–C(4) | 1.37(2) |
| C(4)–C(5) | 1.37(2) | C(5)–C(6) | 1.36(1) |
| P(1)–Ru(1)–P(2) | 97.32(9) | P(1)–Ru(1)–P(3) | 95.0(1) |
| P(1)–Ru(1)–P(4) | 95.9(1) | P(1)–Ru(1)–O(1) | 86.4(2) |
| P(1)–Ru(1)–O(2) | 176.3(2) | Ru(1)–O(1)–C(1) | 126.3(5) |
| Ru(1)–O(2)–C(7) | 130.3(5) | C(6)–O(4)–C(8) | 115.2(9) |
| 2h | | | |
| Ru(1)–P(1) | 2.378(2) | Ru(1)–P(2) | 2.285(1) |
| Ru(1)–P(3) | 2.283(1) | Ru(1)–P(4) | 2.360(2) |
| Ru(1)–O(1) | 2.115(3) | Ru(1)–O(2) | 2.116(3) |
| O(1)–C(1) | 1.311(5) | O(2)–C(7) | 1.280(6) |
| O(3)–C(7) | 1.237(6) | C(1)–C(2) | 1.430(6) |
| C(1)–C(6) | 1.443(6) | C(2)–C(3) | 1.411(6) |
| C(2)–C(7) | 1.492(7) | C(3)–C(4) | 1.361(9) |
| C(4)–C(5) | 1.374(8) | C(5)–C(6) | 1.369(7) |
| P(1)–Ru(1)–P(2) | 95.81(5) | P(1)–Ru(1)–P(3) | 92.91(4) |
| P(1)–Ru(1)–P(4) | 168.27(5) | P(1)–Ru(1)–O(1) | 86.1(1) |
| P(1)–Ru(1)–O(2) | 86.34(10) | O(1)–Ru(1)–O(2) | 86.5(1) |
| Ru(1)–O(1)–C(1) | 127.7(3) | Ru(1)–O(2)–C(7) | 131.9(3) |
| O(2)–C(7)–O(3) | 120.5(5) | O(2)–C(7)–C(2) | 121.9(4) |
| 2j | | | |
| Ru(1)–P(1) | 2.362(1) | Ru(1)–P(2) | 2.437(2) |
| Ru(1)–P(3) | 2.2761(9) | Ru(1)–P(4) | 2.359(2) |
| Ru(1)–O(1) | 2.134(2) | Ru(1)–C(7) | 2.047(4) |
| O(1)–C(1) | 1.311(4) | O(2)–C(7) | 1.227(4) |
| C(1)–C(2) | 1.406(5) | C(1)–C(6) | 1.418(4) |
| C(2)–C(3) | 1.399(5) | C(2)–C(7) | 1.509(5) |
| C(3)–C(4) | 1.361(7) | C(4)–C(5) | 1.380(7) |
| C(5)–C(6) | 1.390(6) | | |
| P(1)–Ru(1)–P(2) | 93.41(6) | P(1)–Ru(1)–P(3) | 95.98(4) |
| P(1)–Ru(1)–P(4) | 166.93(3) | P(1)–Ru(1)–O(1) | 84.91(7) |
| P(1)–Ru(1)–C(7) | 84.7(1) | O(1)–Ru(1)–C(7) | 81.8(1) |
| Ru(1)–O(1)–C(1) | 112.3(2) | Ru(1)–C(7)–O(2) | 132.0(3) |
| Ru(1)–C(7)–C(2) | 109.4(2) | | |

and methyl 3-methylsalicylate (160.0 μL , 1.546 mmol) in benzene (4.0 mL) at 70 °C for 7 days followed by workup involving recrystallization from cold acetone gave pale yellow microcrystals of **2h** in 19% yield (39.4 mg, 0.0709 mmol). This compound was characterized spectroscopically. ^1H NMR (CD_2Cl_2): δ 1.24 (vt, J = 3.0 Hz, 18H, PMe_3), 1.42 (d, J = 8.6 Hz, 18H, PMe_3), 2.06 (s, 3H, Me), 6.17 (dd, J = 7.9, 6.9 Hz, 1H, C_6H_3), 6.92 (dt, J = 6.9, 1.5 Hz, 1H, C_6H_3), 7.83 (dd, J = 7.9 Hz, 1.5 Hz, 1H). $^{31}\text{P}\{^1\text{H}\}$ NMR (CD_2Cl_2): δ 0.80 (t, J = 32 Hz, 2P), 11.8 (q, J = 32 Hz, 1P), 15.0 (q, J = 32 Hz, 1P). IR (KBr, cm^{-1}): 2958(w), 2906(w), 1598(s), 1571(s), 1543(w), 1451(s), 1427(s), 1349(w), 1262(w), 1079(m), 944(s).

cis-Ru[OC₆H₃(CO-2)(OMe-6)- $\kappa^2\text{O},\text{C}$](PMe₃)₄ (2i). Treatment of **1** (109.6 mg, 0.3475 mmol) with PMe_3 (150.0 μL , 1.450 mmol) and 2-hydroxy-3-methoxybenzaldehyde (54.6 mg, 0.359 mmol) in benzene (5.0 mL) at 50 °C for 27 h followed by workup involving recrystallization from cold acetone/hexane gave yellow microcrystals of **2i** in 18% yield (33.2 mg, 0.0632 mmol). ^1H NMR (C_6D_6): δ 0.97 (vt, J = 3.2 Hz, 18H, PMe_3), 1.10 (d, J = 4.5 Hz, 9H, PMe_3), 1.20 (d, J = 7.2 Hz, 9H, PMe_3), 3.83 (s, 3H, OMe), 6.61 (t, J = 7.2 Hz, 1H, C_6H_3), 6.88 (d, J = 7.2 Hz, 1H, C_6H_3), 7.83 (d, J = 7.2 Hz, 1H, C_6H_3). $^{31}\text{P}\{^1\text{H}\}$ NMR (C_6D_6): δ -20.3 (t, J = 26 Hz, 1P), -5.4 (dd, J = 35, 27 Hz, 2P), 11.0 (t, J = 35 Hz, 1P). IR (KBr, cm^{-1}): 3046(w), 2968(w), 2905(m), 2825(w), 1602(w), 1585(w), 1547(s), 1477(m), 1438(m), 1300(m), 1275(w), 1235(m), 1190(m), 1152(w), 1066(w), 943(vs), 916(sh), 852(m), 799(m), 737(m), 714(m), 677(m). Anal. Calcd for $\text{C}_{20}\text{H}_{42}\text{O}_3\text{P}_4\text{Ru}$: C, 43.24; H, 7.62. Found: C, 43.54; H, 7.94.

Table 4. BDEs for Related Bonds in Reported Compounds²⁷

| bond | BDE (kJ mol ⁻¹) | corresponding broken bond in this and previous works |
|-------------------------------------|-----------------------------|---|
| MeC(O)–NH ₂ | 417.1 \pm 8.4 | |
| PhC(O)–OMe | 409 \pm 12.6 | |
| PhC(O)–H | 371 \pm 10.9 | HOC ₆ H ₃ (R-6)[C(O)–H-2] |
| PhCH ₂ –H | 370.3 \pm 6.3 | HOC ₆ H ₃ (R-6)(CH ₂ –H-2) |
| MeC(O)O–Me | 352.7 \pm 5.0 | HOC ₆ H ₃ (R-6)[C(O)O–Me-2] |
| PhS–Me | 278.2 \pm 10.5 | |
| PhO–Me | 268.6 \pm 7.1 | HOC ₆ H ₃ (R-6)(O–Me-2) |
| PhCH ₂ –NMe ₂ | 259.8 \pm 8.4 | |

cis-Ru[OC₆H₃(CO-2)(Me-6)- $\kappa^2\text{O},\text{C}$](PMe₃)₄ (2j). Treatment of **1** (103.8 mg, 0.3291 mmol) with PMe_3 (140.0 μL , 1.353 mmol) and 2-hydroxy-3-methylbenzaldehyde (40.0 μL , 0.330 mmol) in benzene (5.0 mL) at 70 °C for 4 days followed by workup involving recrystallization from cold toluene gave pale orange crystals of **2j** in 26% yield (46.1 mg, 0.0854 mmol). ^1H NMR (C_6D_6): δ 0.93 (vt, J = 2.7 Hz, 18H, PMe_3), 1.18 (d, J = 4.8 Hz, 9H, PMe_3), 1.21 (d, J = 7.2 Hz, 9H, PMe_3), 2.53 (s, 3H, Me), 6.67 (t, J = 7 Hz, 1H, C_6H_3), 7.24 (d, J = 6.3 Hz, 1H, C_6H_3), 7.98 (d, J = 7.2 Hz, 1H, C_6H_3). $^{31}\text{P}\{^1\text{H}\}$ NMR (C_6D_6): δ -20.1 (t, J = 26 Hz, 1P), -5.4 (dd, J = 35, 26 Hz, 2P), 10.7 (t, J = 35 Hz, 1P). Anal. Calcd for $\text{C}_{20}\text{H}_{42}\text{O}_2\text{P}_4\text{Ru}$: C, 44.52; H, 7.85. Found: 43.36; H, 7.81.

cis-Ru[OC₆H₄(SMe-2)- $\kappa^2\text{O},\text{S}$][OC₆H₄(SMe-2)- $\kappa^1\text{O}$](PMe₃)₃ (3). Treatment of **1** (250.1 mg, 0.7929 mmol) with PMe_3 (320.0 μL , 3.091 mmol) and 2-hydroxythioanisole (210.0 μL , 1.616 mmol) in benzene (5.0 mL) at 70 °C for 5 days followed by workup involving recrystallization from cold acetone gave colorless microcrystals of **3** in 28% yield (136.3 mg, 0.2243 mmol). ^1H NMR (C_6D_6): δ 0.74 (d, J = 8.4 Hz, 9H, PMe_3), 1.24 (d, J = 9.0 Hz, 9H, PMe_3), 1.29 (d, J = 8.7 Hz, 9H, PMe_3), 2.19 (s, 3H, SMe), 2.29 (d, J = 2.7 Hz, 3H, SMe), 5.48 (ddd, J = 8.7, 5.4, 2.1 Hz, 1H, C_6H_4), 6.68 (td, J = 7.3, 1.2 Hz, 1H, C_6H_4), 6.82 (dd, J = 7.3, 2.1 Hz, 1H, C_6H_4), 7.7 (m, 4H, C_6H_4), 7.79 (dd, J = 8.7, 1.2 Hz, 1H, C_6H_4). $^{31}\text{P}\{^1\text{H}\}$ NMR (C_6D_6): δ 14.0 (dd, J = 39, 32 Hz, 1P), 15.5 (t, J = 39 Hz, 1P), 17.4 (dd, J = 38, 32 Hz, 1P). Anal. Calcd for $\text{C}_{23}\text{H}_{41}\text{O}_2\text{P}_3\text{S}-\text{RuS}_2$: C, 45.46; H, 6.80; S, 10.55. Found: C, 45.95; H, 6.88; S, 10.85.

cis-[Ru{OC₆H₄(CONH₂-2)- $\kappa^2\text{O},\text{O}'$ }(PMe₃)₄]⁺[OC₆H₄(CONH₂-2)]⁻ (4). Treatment of **1** (112.7 mg, 0.3573 mmol) with PMe_3 (150.0 μL , 1.445 mmol) and 2-hydroxybenzamide (40.0 μL , 0.0534 mmol) in benzene (5.0 mL) at 50 °C for 3 days followed by workup involving recrystallization from cold acetone gave colorless microcrystals of **4** in 42% yield (102.2 mg, 0.1508 mmol). This compound was characterized spectroscopically. ^1H NMR (CD_3COCD_3): δ 1.26 (vt, J = 3.3 Hz, 18H, PMe_3), 1.38 (d, J = 7.2 Hz, 9H, PMe_3), 1.51 (d, J = 8.1 Hz, 9H, PMe_3), 6.19 (t, J = 7.2 Hz, 1H, C_6H_4), 6.46 (d, J = 8.1 Hz, 1H, C_6H_4), 6.71 (t, J = 7.4 Hz, 1H, C_6H_4), 6.89 (t, J = 7.4 Hz, 1H, C_6H_4), 7.01 (d, J = 8.1 Hz, 1H, C_6H_4), 7.26 (t, J = 7.2 Hz, 1H, C_6H_4), 7.99 (d, J = 7.5 Hz, 1H, C_6H_4), 8.06 (d, J = 8.4 Hz, 1H). $^{31}\text{P}\{^1\text{H}\}$ NMR (CD_3COCD_3): δ 0.2 (t, J = 31 Hz, 2P), 4.1 (q, J = 31 Hz, 1P), 10.4 (q, J = 31 Hz, 1P). IR (KBr, cm^{-1}): 3311(s), 3137(m), 3044(m), 2972(m), 2911(s), 1714(w), 1656(vs), 1599(vs), 1558(vs), 1524(s), 1460(vs), 1368(s), 1347(s), 1306(s), 1285(m), 1252(m), 1134(m), 1083(w), 1032(m), 943(vs), 877(s), 855(vs), 753(vs), 718(vs), 666(vs), 537(s).

cis-RuH[OC₆H₄(CH₂NMe₂-2)](PMe₃)₄ (5). Treatment of **1** (82.0 mg, 0.260 mmol) with PMe_3 (110.0 μL , 1.060 mmol) and 2-*N,N*-dimethylaminomethylphenol (40.0 μL , 0.265 mmol) in benzene (5.5 mL) at 70 °C for 5 days followed by workup involving recrystallization from cold acetone gave light brown microcrystals of **5** in 26% yield (37.5 mg, 0.0675 mmol). ^1H NMR (CD_3COCD_3): δ -7.83 (dq, J = 102, 27 Hz, 1H, RuH), 1.30 (vt, J = 2.7 Hz, 18H, PMe_3), 1.37 (d, J = 8.1 Hz, 9H, PMe_3), 1.46 (d, J = 5.4 Hz, 9H, PMe_3), 2.11 (s, 6H, NMe_2), 3.25 (s, 2H, CH_2), 6.05 (t, J = 7.8 Hz, 1H, C_6H_4), 6.80 (t, J = 6.3 Hz, 1H, C_6H_4), 6.91 (d, J = 7.5 Hz,

1H, C₆H₄), 7.24 (d, *J* = 8.4 Hz, 1H, C₆H₄). ³¹P{¹H} NMR (CD₃-COCD₃): δ −11.8 (td, *J* = 27, 17 Hz, 1P), 1.5 (dd, *J* = 33, 27 Hz, 2P), 16.1 (td, *J* = 33, 17 Hz, 1P). IR (KBr, cm^{−1}): 3437(w), 2964(m), 2901(m), 2847(w), 2804(w), 2761(w), 2707(w), 1847(m), 1587(m), 1474(s), 1446(m), 1361(w), 1330(m), 1305(m), 1278(m), 1177(w), 1144(w), 1012(w), 941(vs), 855(m), 749(m), 711(m), 664(m), 581(w). Anal. Calcd for C₂₁H₄₉NOP₄Ru: C, 45.32; H, 8.87; N, 2.52. Found: C, 45.26; H, 8.79; N, 2.00.

Protonolysis of 2a with HCl. Complex **2a** (23.3 mg, 0.0454 mmol) was placed in an NMR tube into which C₆D₆ (0.6 mL) was introduced by vacuum distillation. By use of a mercury manometer, dry hydrogen chloride (4.97 mL, 0.20 mmol) was added into the NMR tube. ¹H NMR analysis of the product showed formation of catechol in 97% yield.

Hydrogenolysis of 2a. Complex **2a** (10.2 mg, 0.0192 mmol) and triphenylmethane as an internal standard were placed in an NMR tube into which acetone-*d*₆ (0.6 mL) was introduced by vacuum distillation. The NMR tube was placed in a stainless autoclave, then H₂ (6.8 MPa) was charged. The autoclave was heated at 70 °C for 20 h. An ¹H NMR spectrum of the product showed formation of *cis*-RuH₂(PMe₃)₄ in 32% and catechol in 33% yield.

Protonolysis of 2d with HCl. Complex **2d** (15.3 mg, 0.0282 mmol) was placed in an NMR tube into which CDCl₃ (0.6 mL) was introduced by vacuum distillation. After exposure of the solution to dry hydrogen chloride for 10 min, 1,4-dioxane was added as an internal standard, and the ¹H NMR spectrum showed formation of salicylic acid in 100% yield.

Treatment of 3 with PMe₃. Complex **3** (12.2 mg, 0.0201 mmol) was placed in an NMR tube into which a flame-sealed capillary containing a C₆D₆ solution of P(OPh)₃ as an external standard and toluene-*d*₈ (0.6 mL) were added under N₂ atmosphere. PMe₃ (3.2 μL, 0.031 mmol) was added to the solution by hypodermic syringe and then heated at 100 °C for 60 h. Formation of *trans*-Ru[OC₆H₄-(SMe-2)-*κ*²O,*S*]₂(PMe₃)₂ (**6**) was observed in 85% yield. **6**: ¹H NMR (C₆D₅CD₃): δ 0.90 (distorted vt, *J* = 3 Hz, 18H, PMe₃), 2.53 (s, 6H, SMe), 6.47 (td, *J* = 8, 1 Hz, 2H, C₆H₄), 6.76 (t, *J* = 8 Hz, 2H, C₆H₄), 7.24 (dd, *J* = 8, 1 Hz, 2H, C₆H₄) and 2H due to aromatic protons were obscured by concomitant P(OPh)₃. ³¹P{¹H} NMR (C₆D₅CD₃): δ 15.3 (s).

Time-Course for the Reaction of 1/PMe₃ with Methyl Salicylate. Complex **1** (12.5 mg, 0.0396 mmol) was placed in an NMR tube into which C₆D₆ (0.6 mL) was added by vacuum distillation. A flame-sealed capillary containing a C₆D₆ solution of P(OPh)₃ was added in the NMR tube as an external standard. PMe₃ (16.0 μL, 0.155 mmol) and methyl salicylate (10.0 μL, 0.0772 mmol) were added by hypodermic syringe, and then the reaction system was heated at 70 °C.

Time-Course for the Reaction of 8/PMe₃ with Methyl Salicylate. (A) Complex **8** (17.3 mg, 0.0410 mmol) was placed in an NMR tube into which C₆D₆ (0.60 mL) was introduced by vacuum distillation. A flame-sealed capillary containing a C₆D₆ solution of P(OPh)₃ was added in the NMR tube as an external standard. PMe₃ (7.4 μL, 0.0715 mmol) and methyl salicylate (14.5 μL, 0.112 mmol) were added to the NMR tube by hypodermic syringe, and then the reaction mixture was heated at 70 °C. The following experiments were also carried out in a similar way. (B) **8** (17.6 mg, 0.0148 mmol), C₆D₆ (0.60 mL), PMe₃ (40.0 μL, 0.386 mmol), and methyl salicylate (14.5 μL, 0.112 mmol). (C) **8** (17.3 mg, 0.0410 mmol), C₆D₆ (0.6 mL), PMe₃ (38.0 μL, 0.367 mmol), and methyl salicylate (48.0 μL, 0.370 mmol). (D) **8** (8.3 mg, 0.020 mmol), C₆D₆ (0.6 mL), PMe₃ (16.5 μL, 0.159 mmol), and methyl salicylate (6.6 μL, 0.051 mmol). (E) **8** (17.3 mg, 0.0410 mmol), DMSO-*d*₆ (0.6 mL), PMe₃ (38.5 μL, 0.372 mmol), and methyl salicylate (12.0 μL, 0.109 mmol). (F) **8** (8.7 mg, 0.021 mmol), C₆D₆ (0.6 mL), PMe₃ (17.5 μL, 0.169 mmol), and methyl 5-fluorosalicylate (9.2 mg, 0.054 mmol). (G) **8** (8.7 mg, 0.021 mmol), C₆D₆ (0.6 mL), PMe₃ (17.5

Table 5. Crystallographic Parameters for 2a, 2c, 2g, 2h, 2j, 3, and 9

| | 2a | 2c | 2g | 2h | 2j | 3 | 9 |
|----------------------------------|--|---|--|--|--|---|---|
| formula | C ₁₈ H ₄₀ O ₂ P ₄ Ru | C ₁₀ H ₃₉ NO ₄ P ₄ Ru | C ₂₀ H ₄₂ O ₄ P ₄ Ru | C ₂₀ H ₄₂ O ₃ P ₄ Ru | C ₂₀ H ₄₂ O ₂ P ₄ Ru | C ₂₃ H ₄₁ O ₂ P ₃ S ₂ Ru | C ₁₇ H ₃₉ P ₃ Ru |
| fw | 513.48 | 570.49 | 571.51 | 555.52 | 539.52 | 607.69 | 437.49 |
| cryst syst | monoclinic | monoclinic | tetragonal | orthorhombic | monoclinic | triclinic | orthorhombic |
| space group | P ₂ /a (No. 14) | P ₂ /a (No. 4) | P ₄ 2/c (No. 114) | P ₂ 1 ₂ 1 ₂ 1 (No. 61) | P ₂ /n (No. 14) | P ₁ (No. 2) | P ₂ 1 ₂ 1 ₂ (No. 62) |
| <i>a</i> (Å) | 14.110(6) | 13.847(3) | 17.307(6) | 17.67(1) | 10.25(1) | 10.000(1) | 12.52(1) |
| <i>b</i> (Å) | 12.546(3) | 12.407(7) | 17.307(6) | 20.02(1) | 18.88(1) | 15.722(3) | 13.60(1) |
| <i>c</i> (Å) | 14.528(4) | 14.779(10) | 18.18(1) | 15.035(9) | 14.02(1) | 9.152(2) | 12.60(1) |
| <i>a</i> (deg) | 90 | 90 | 90 | 90 | 90 | 93.52(2) | 90 |
| <i>β</i> (deg) | 102.77(3) | 90.04(3) | 90 | 101.06(7) | 101.06(7) | 108.89(1) | 90 |
| <i>γ</i> (deg) | 90 | 90 | 90 | 90 | 90 | 87.62(1) | 90 |
| <i>V</i> (Å ³) | 2508(1) | 2539(1) | 5446(3) | 5318(3) | 2664(3) | 1358.3(4) | 2145(6) |
| <i>Z</i> | 4 | 4 | 8 | 8 | 4 | 2 | 4 |
| temp (K) | 243.2 | 200.2 | 293.2 | 293.2 | 293.2 | 200.2 | 200.2 |
| cryst size (mm) | 0.61 × 0.43 × 0.17 | 0.73 × 0.48 × 0.38 | 0.30 × 0.20 × 0.10 | 0.83 × 0.83 × 0.50 | 0.65 × 0.20 × 0.15 | 0.37 × 0.25 × 0.12 | 0.20 × 0.20 × 0.20 |
| total no. of reflns | 4757 | 6115 | 3434 | 6114 | 6122 | 6144 | 2162 |
| no. of refined reflns | 2546 | 5682 | 2637 | 4220 | 4742 | 4478 | 1912 |
| no. of params | 227 | 525 | 262 | 252 | 244 | 279 | 104 |
| <i>R</i> , <i>R</i> _w | 0.0380, 0.0497 | 0.0688, 0.1130 | 0.0494, 0.0676 | 0.0455, 0.0673 | 0.0349, 0.0487 | 0.0794, 0.1571 | 0.0291, 0.0600 |
| GOF | 1.122 | 1.133 | 1.083 | 1.110 | 1.333 | 1.542 | 0.824 |

μL , 0.169 mmol), and methyl 5-methoxysalicylate (8.0 μL , 0.054 mmol). (H) **8** (8.6 mg, 0.020 mmol), C_6D_6 (0.6 mL), PMe_3 (16.5 μL , 0.159 mmol), and methyl 4-methoxysalicylate (9.4 mg, 0.052 mmol). (I) **8** (8.5 mg, 0.020 mmol), C_6D_6 (0.6 mL), PMe_3 (23.0 μL , 0.222 mmol), and isopropyl salicylate (11.0 μL , 0.0665 mmol).

Characterization of 9. During the course of the reaction of **1** with PMe_3 and methyl salicylate, $\text{Ru}(6-\eta^1:1-3-\eta^3-\text{C}_8\text{H}_{12})(\text{PMe}_3)_3$ (**9**) was observed by NMR spectroscopy. ^1H NMR (C_6D_6): δ 0.68 (d, $J = 4.8$ Hz, 9H, PMe_3), 1.24 (d, $J = 6.3$ Hz, 18H, PMe_3), 1.8–2.4 (m), 3.62 (dt, $J = 18.3, 7.2$ Hz, 1H, *central CH* in the allylic moiety), 3.94 (m, 2H, allylic CH). $^{31}\text{P}\{^1\text{H}\}$ NMR (C_6D_6): δ –13.6 (t, $J = 26$ Hz, 1P), –2.20 (d, $J = 26$ Hz, 2P). By an independent reaction, crystals of **9** suitable for X-ray analysis were obtained by fractional crystallization from cold acetone. The molecular structure of **9** is depicted in Figure 8. The overall structure of **9** is basically close to that of **8**, but **9** has C_s symmetry in its molecule. The crystallographic data are deposited in the Supporting Information.

Reaction of *trans*- $\text{RuCl}_2(\text{PMe}_3)_4$ (12**) with Potassium Salt of Methyl Salicylate or Potassium 2,6-Dimethoxyphenoxide in THF.** *trans*- $\text{RuCl}_2(\text{PMe}_3)_4$ (**12**) (11.1 mg, 0.0233 mmol) and potassium salt of methyl salicylate (16.9 mg, 0.0888 mmol) were placed in a Schlenk tube into which dry THF (1.0 mL) was introduced. The reaction mixture was heated at 70 °C for 4 days. After removal of all volatile matters, the resulting product was dried under reduced pressure. The product was dissolved in CD_2Cl_2 , and triphenylmethane was added as an internal standard. The NMR measurement of this product showed formation of **2d** in 65% and methyl 2-methoxybenzoate in 7% yield. Similar treatment of **12** (11.2 mg, 0.0235 mmol) with potassium 2,6-dimethoxyphenoxide (14.8 mg, 0.0770 mmol) at 70 °C for 4 days produced **2e** in 61% and 1,2,3-trimethoxybenzene in 7% yield.

Reaction of 12 with Potassium Salt of Methyl Salicylate in DME. Complex **12** (10.2 mg, 0.0214 mmol) and potassium salt of methyl salicylate (12.8 mg, 0.0673 mmol) were placed in a Schlenk tube. Dry DME (1.5 mL) was added into the Schlenk tube by syringe, and the suspension was heated at 70 °C for 3 days. No formation of methyl 2-methoxybenzoate was confirmed by GLC analysis of the solution. After removal of all volatile matters, products were extracted with dichloromethane- d_2 and the NMR spectrum showed formation of **2d** in 10% yield and a new species

having an ABX spin system (intermediate **C**) in 68% yield in the $^{31}\text{P}\{^1\text{H}\}$ NMR (Ph_3CH was used as an internal standard). Intermediate **C**: $^{31}\text{P}\{^1\text{H}\}$ NMR (CD_2Cl_2): δ 30.5 (dd, $J = 44, 39$ Hz, 1P), 27.0 (dd, $J = 44, 39$ Hz, 1P), 22.6 (t, $J = 39$ Hz, 1P). Immediately after addition of PMe_3 (2 μL , 0.02 mmol) into the mixture, **2d** (16%) and a new species having an AMX₂ spin system (intermediate **D**) (56%) were produced. Intermediate **D**: $^{31}\text{P}\{^1\text{H}\}$ (CD_2Cl_2): δ 19.9 (q, $J = 34$ Hz, 1P), 12.4 (q, $J = 34$ Hz, 1P), –1.43 (t, $J = 34$ Hz, 2P). Then, the solvent was removed under reduced pressure and benzene- d_6 was introduced into the NMR tube. Heating of this system at 70 °C for 30 min gave a mixture of **2d** (76%) and **D** (16%). Methyl 2-methoxybenzoate was not observed at all.

X-ray Structure Determination. A summary of crystallographic data for **2a**, **2c**, **2g**, **2h**, **2j**, **3**, and **9** is given in Table 5. Data collection was carried out on a Rigaku AFC-7R diffractometer using graphite-monochromated Mo K α radiation ($\lambda = 0.7107$ Å). A selected yellow crystal was mounted on a glass fiber with Paratone N oil or in a capillary tube (glass, 0.7 mm ϕ), which was sealed by small flame torch. The structure was solved by the direct methods (SIR88)³³ or Paterson method with the teXsan program package³⁴ and refined by full-matrix least-squares cycles. Absorption corrections were applied by the ϕ -scan method. Hydrogen atoms were placed in calculated positions, but they were not refined. Crystallographic thermal parameters and bond distances and angles have been deposited as Supporting Information.

Acknowledgment. This study was financially supported by the Ministry of Education, Culture, Sports, Science and Technology, Japan. The authors thank Mr. S. Kanaya for characterization of **9** and Ms. S. Kiyota for elemental analyses.

Supporting Information Available: Full description of crystallographic data for **2a**, **2c**, **2g**, **2h**, **2j**, **3**, and **9**. This material is available free of charge via the Internet at <http://pubs.acs.org>.

OM061183M

(33) Burla, M. C.; Camalli, M.; Cascarano, G.; Giacovazzo, C.; Polidori, G.; Spagna, R.; Viterbo, D. *J. Appl. Cryst.* **1989**, 22, 389.

(34) Crystal Structure Analysis Package, Molecular Structure Corporation (1985 and 1999)